

**SIGNAL AND IMAGE DENOISING USING DISCRETE
WAVELET TRANSFORM BASIS FUNCTION**

by

MOHD NUR AMIN BIN HASHIM

DISSERTATION

Submitted to the Electrical & Electronics Engineering Programme
in Partial Fulfillment of the Requirements
for the Degree
Bachelor of Engineering (Hons)
(Electrical & Electronics Engineering)

Universiti Teknologi PETRONAS

Bandar Seri Iskandar

31750 Tronoh

Perak Darul Ridzuan

© Copyright 2010

by

Mohd Nur Amin Bin Hashim, 2010

CERTIFICATION OF APPROVAL

SIGNAL AND IMAGE DENOISING USING DISCRETE WAVELET TRANSFORM BASIS FUNCTION

by

MOHD NUR AMIN BIN HASHIM

A project dissertation submitted to the
Electrical & Electronics Engineering Programme
Universiti Teknologi PETRONAS
in partial fulfilment of the requirement for the
Bachelor of Engineering (Hons)
(Electrical & Electronics Engineering)

Approved:

MR. SAMSUL ARIFFIN BIN ABDUL KARIM
Project Supervisor

UNIVERSITI TEKNOLOGI PETRONAS

TRONOH, PERAK

December 2010

CERTIFICATION OF ORIGINALITY

This is to certify that I am responsible for the work submitted in this project, that the original work is my own except as specified in the references and acknowledgements, and that the original work contained herein have not been undertaken or done by unspecified sources or persons.

Mohd Nur Amin Bin Hashim

ABSTRACT

Wavelet transform is being used quite extensively in mathematical sciences and engineering problems notably in image compression and image de-noising. Given any signal with noise, our main objective is to remove the noise and reconstruct the original signal with an acceptable error. This objective can be achieved by using threshold method. In denoising, we can utilize both threshold methods i.e. hard and soft thresholding. Comparative study was done using root mean square error (RMSE) and signal-to-noise ratio (SNR) as measurements to the quality of denoised signal as compared to the original signal. In this paper, we applied two types of wavelet i.e. Haar and Daubechies 4 (Db4) wavelets to denoise various types of signal with noise. In addition, data from Kuala Lumpur Composite Index (KLCI) and Electrocardiography (ECG) were used to show how denoising being applied to real data. Based on numerical results, it was found that both methods are capable to denoise all signals with an acceptable RMSE and SNR. We also showed that for certain signals, Haar wavelet is better than Db4 wavelet and vice versa. For the image denoising, the objective is quite the same but different approach is taken. Three types of noise are applied on the tested images and denoising is done using a global thresholding rule for both Haar and Daubechies 4 wavelets. PSNR and RMSE become the comparative tools to determine which wavelet is better in image denoising.

ACKNOWLEDGMENT

First and foremost, praise to Allah the Almighty, who has helped and gave me courage and strength in completing Final Year Project (FYP). Without His blessing, this FYP will not be a success. I would like to take this opportunity to express my deepest gratitude to anyone that involved in this project ranging from UTP lecturers, friends and to my family who have been supportive in helping me doing the project.

I am profoundly grateful to my supervisor, Mr. Samsul Ariffin Bin Abdul Karim who has guided and given me opportunity to handle the project. Last but not least, many thanks to others whose name was not mentioned in this page but has in one way or another contributed to the accomplishment of this project.

TABLE OF CONTENTS

CERTIFICATION OF APPROVAL	II
CERTIFICATION OF ORIGINALITY.....	III
ABSTRACT	IV
ACKNOWLEDGMENT	V
LIST OF FIGURES	IX
LIST OF TABLES	XII
CHAPTER 1	1
1.1 Background of Study	1
1.2 Problem Statement	2
1.3 Objectives.....	2
1.4 Scope of Study	2
1.4.1 <i>Discrete Wavelet Transform</i>	2
1.4.2 <i>Signal (1-Dimension)</i>	3
1.4.2 <i>Image (2-Dimension)</i>	3
CHAPTER 2	4
2.1 Wavelet transform.....	4
2.2 Wavelet Family	5
2.3. Discrete Wavelet Transform	6
2.3.1 <i>One Dimensional data (Signal)</i>	7
2.3.2 <i>Two Dimensional data</i>	10
2.4 Denoising Method.....	12
2.4.1 <i>Hard Thresholding</i>	13
2.4.2 <i>Soft Thresholding</i>	14

2.4.2	<i>VisuShrink</i>	14
2.4.3	<i>Rigrsure</i>	15
2.4.4	<i>Heursure</i>	15
2.5	Noise	16
2.5.1	<i>Gaussian noise</i>	16
2.5.2	<i>Salt and pepper noise</i>	17
2.5.3	<i>Speckle noise</i>	18
2.6	Electrocardiography (ECG)	19
2.7	Comparative study measurement	20
2.7.1	<i>One-dimensional data</i>	21
2.7.2	<i>Two-dimensional data</i>	21
CHAPTER 3	22
3.1	Procedure identification	22
3.2	Data	23
3.3	Denoising	24
3.3.1	<i>Signal Denoising</i>	24
3.3.2	<i>Image denoising</i>	25
3.4	Tools.....	25
CHAPTER 4	26
4.1	Results	26
4.1.1	<i>Signal denoising</i>	26
4.1.2	<i>Image denoising</i>	40
4.1.3	<i>Kuala Lumpur Composite Index Data (KLCI)</i>	66
4.1.4	<i>Electrocardiography data (ECG)</i>	71
4.2	Discussions.....	75
4.2.1	<i>Signal denoising</i>	75
4.2.2	<i>Image denoising</i>	76
4.2.3	<i>Kuala Lumpur Composite Index Data (KLCI)</i>	76

4.2.4 <i>Electrocardiography data (ECG)</i>	77
CHAPTER 5	78
5.1 Conclusion	78
5.1.1 <i>Signal</i>	78
5.1.2 <i>Image</i>	78
5.2 Recommendation.....	79
REFERENCES	80
APPENDICES	83
APPENDIX A	84

LIST OF FIGURES

Figure 1: Wavelet families (a) Haar (b) Daubechies4 (c) Coiflet1 (d) Symlet2 (e)Meyer (f) Morlet (g) Mexican Hat.....	6
Figure 2 : Decomposition of One Dimensional data [11].....	7
Figure 3 : Mallat's decomposition tree [11]	8
Figure 4 : Reconstruction of One Dimensional data [11]	9
Figure 5 : Decomposition of 2-Dimensional data (Image) [11].....	10
Figure 6: Reconstruction of 2-Dimensional data [11].....	11
Figure 7 : Two level of Mallat's Decomposition Trees (Image) [11]	11
Figure 8 : Three level of Mallat's Decomposition Trees (Image)	12
Figure 9 : Hard Thresholding	13
Figure 10 : Soft Thresholding	14
Figure 11 : Gaussian Noise with variance 0.05 [12].....	17
Figure 12 : Speckle Noise with variance 0.05 [12].....	18
Figure 13 : Speckle noise with 0.0.5 variance [12].....	19
Figure 14 : 12 Lead ECG of a 26-year-old male. [18].....	20
Figure 15 : Flow chart of thesis	22
Figure 16 : Flow chart of signal denoising	24
Figure 17 : Flow chart of image denoising	25
Figure 18 : SNR vs. level for blocks signal	32
Figure 19 : SNR vs. level for bumps signal	33
Figure 20 : SNR vs. level for heavy sine signal.....	34
Figure 21: Haar wavelet transform at level 10 using Soft thresholding Rigrsure .	36
Figure 22 Haar wavelet transform at level 10 using Soft Thresholding Heursure .	36
Figure 23 : Haar wavelet transform at level 10 using Hard Thresholding Heursure	37
Figure 24 : Haar wavelet transform at level 10 using Hard Thresholding Rigrsure	37

Figure 25 : Db4 wavelet transform at level 8 using soft thresholding, Heuresure...	38
Figure 26 : Db4 wavelet transform at level 8 using soft thresholding, Rigrsure ..	38
Figure 27 :Db4 wavelet transform at level 8 using hard thresholding, Heuresure .	39
Figure 28 : Db4 wavelet transform at level 8 using hard thresholding, Rigrsure .	39
Figure 29 : PSNR vs. Images for Gaussian noise	44
Figure 30 : PSNR vs. Image for Salt and Pepper noise	45
Figure 31: PSNR vs. Image for Speckle noise	46
Figure 32 : Barbara corrupted with Gaussian noise at variance 0.05.....	47
Figure 33 Denoised Barbara using Db4 at level 3	48
Figure 34 : Barbara corrupted with Salt and Pepper noise at variance 0.05	48
Figure 35 : Denoised Barbara using Haar at level 2	49
Figure 36 : Barbara corrupted with Speckle noise at variance 0.05.....	49
Figure 37 : Denoised Barbara using Haar at level 2	50
Figure 38 : Mandrill corrupted with Gaussian noise at variance 0.05	51
Figure 39 : Denoised Mandrill using Db4 at level 2.....	51
Figure 40 : Mandrill corrupted with Salt and Pepper noise at variance 0.05.....	52
Figure 41: Denoised Mandrill using Haar at level 2	52
Figure 42: Mandrill corrupted with Speckle noise at variance 0.05	53
Figure 43 : Denoised Mandrill using Db4 at level 1	53
Figure 44 : Airplane corrupted with Gaussian noise at variance 0.05	54
Figure 45 : Denoised Airplane using Db4 at level 3.....	54
Figure 46 : Airplane corrupted with Salt and Pepper noise at variance 0.05.....	55
Figure 47 : Denoised Airplane using Db4 at level 3.....	55
Figure 48 : Airplane corrupted with Speckle noise at variance 0.05	56
Figure 49 : Denoised Airplane using Haar at level 1	56
Figure 50 : Bridge corrupted with Gaussian noise at variance 0.05	57
Figure 51: Denoised Bridge using Db4 at level 3	57
Figure 52: Bridge corrupted with Salt and Pepper noise at variance 0.05.....	58
Figure 53: Denoised Bridge using Haar at level 3	58
Figure 54 : Bridge corrupted with Speckle noise at variance 0.05	59

Figure 55: Denoised Bridge using Db4 at level 1	59
Figure 56 : Sailboat corrupted with Gaussian noise at variance 0.05	60
Figure 57: Denoised Sailboat using Db4 at level 3.....	60
Figure 58 : Sailboat corrupted with Salt and Pepper noise at variance 0.05.....	61
Figure 59 : Denoised Sailboat using Haar at level 3.....	61
Figure 60: Sailboat corrupted with Speckle noise at variance 0.05	62
Figure 61 : Denoised Sailboat using Db4 at level 2.....	62
Figure 62 : Couple corrupted with Gaussian noise at variance 0.05.....	63
Figure 63 : Denoised Couple using Haar at level 1	63
Figure 64 : Couple corrupted with Salt and Pepper noise at variance 0.05	64
Figure 65 : Denoised Couple using Haar at level 3	64
Figure 66: Couple corrupted with Speckle noise at variance 0.05.....	65
Figure 67 : Denoised Couple using Db4 at level 1	65
Figure 68 : Kuala Lumpur Composite Index	66
Figure 69 : Haar wavelet transform level 1 to level 10.....	68
Figure 70 : Db4 wavelet transform level 1 to level 10.....	69
Figure 71 : The overall RMSE and SNR value vs level	70
Figure 72 : ECG Data.....	71
Figure 73 : Haar wavelet transform of ECG data from level 1 to level 6.....	73
Figure 74 : Db4 wavelet transform of ECG data from level 1 to level 6.....	74

LIST OF TABLES

Table 1 Haar Wavelet Soft Thresholding.....	27
Table 2 Haar Wavelet Hard Thresholding.....	28
Table 3 Db4 Wavelet Soft Thresholding.....	29
Table 4 Db4 Wavelet Hard Thresholding.....	30
Table 5 Overall SNR and RMSE at optimum level.....	31
Table 6 SNR and RMSE for Gaussian with variance 0.05.....	41
Table 7 SNR and RMSE for Salt and Pepper with variance 0.05.....	42
Table 8 SNR and RMSE for Speckle with variance 0.05.....	43
Table 9 SNR and RMSE of data KLCI.....	70
Table 10 SNR and RMSE of ECG data.....	75
Table 11 Overall wavelet performance of signal denoising.....	78
Table 12 Overall wavelet performance of signal denoising.....	79

CHAPTER 1

INTRODUCTION

1.1 Background of Study

The transform of a signal is just another form of representing the signal. It does not change the information content present in the signal. The Wavelet Transform provides a time-frequency representation of the signal. It was developed to overcome the shortcoming of the Short Time Fourier Transform (STFT), which can also be used to analyze non-stationary signals. While STFT gives a constant resolution at all frequencies, The Wavelet Transform uses multi-resolution technique by which different frequencies are analyzed with different resolutions [1]. Unlike basic Fourier analysis, wavelets do not lose completely time information, a feature that makes the technique suitable for applications where the temporal location of the signal's frequency content is important. One of the fields where wavelets have been successfully applied is data analysis. In particular, it has been demonstrated that wavelets produce excellent results in signal denoising i.e. the removal of noise from an unknown signal. Shrinkage methods for noise removal, first introduced by Donoho in 1993, have led to a variety of approaches combining wavelets with probabilistic concepts leading to new efficient denoising procedures [2]. This thesis presents a summary of basic methods for noise removal and their main features and limitations are discussed. A comparative study using data corrupted by noise i.e Gaussian White Noise, Salt and Pepper Noise and Speckle Noise was done and summarized.

1.2 Problem Statement

While there are various methods in image de-noising field, selecting the appropriate methods plays a major role in getting the desired output. Denoising using discrete-wavelet-based approach is one of the popular methods besides other methods such as filtering approach and multifractal approach. In wavelet-based approach, two wavelet basis functions i.e Haar and Daubechies4 are introduced and thresholding method for these two basis functions is applied. In order to quantify the performance of these two wavelet functions, corrupted signals and images with noise i.e. Gaussian White Noise, Salt and Pepper and Speckle were used and comparative study was done using Signal to Noise Ratio (SNR), Root Mean Square Error (RMSE) and Peak Signal to Noise Ratio (PSNR).

1.3 Objectives

The objectives of this project are:

- a. To determine the optimum level of wavelet transformation in signal denoising for both soft and hard thresholding.
- b. To determine the optimum level of wavelet transformation in image denoising for global thresholding.
- c. To determine which wavelet basis function is better in data denoising.

1.4 Scope of Study

1.4.1 Discrete Wavelet Transform

The Discrete Wavelet Transform (DWT), which is based on sub-band coding, gives a fast computation of Wavelet Transform. It is also easy to implement and reduces the computation time and resources required [1]. As compared to

continuous wavelet transform (CWT) that use a set of basis functions with each other by simple scaling and translation, DWT on the other hand uses a digital filtering technique to produce a time-scale representation of the digital data. The calculation of produced coefficients was done using MATLAB.

1.4.2 Signal (1-Dimension)

Three types of signal were used to represent 1-dimensional data. They were blocks, bumps, and heavy sine which were chosen because of their caricature spatially variable function arising in imaging spectroscopy and other scientific signal processing [3]. All the signals were fixed to 1024 points (length) and the comparison was made using SNR and RMSE values. In addition, data from Kuala Lumpur Composite Index (KLCI) and Electrocardiography (ECG) were used to show how denoising being applied to real data.

1.4.2 Image (2-Dimension)

Six grayscale tested images were used to represent 2-dimensional data. They were Barbara, Mandrill, Airplane, Bridge, Couple and Sailboat. These images were fixed to 512x512 resolutions. The comparison was done using PSNR and RMSE.

CHAPTER 2

LITERATURE REVIEW

2.1 Wavelet transform

Basically we define wavelet directly from its counterpart that is scaling function or father wavelet and wavelet function or mother wavelet ([4],[5],[6] & [7]). Suppose that there exist a function $\phi(t) \in L^2(\mathbb{R})$ such that the family of functions [8]

$$\phi_{j,k}(x) = 2^{\frac{j}{2}} \phi(2^j x - k), j, k \in \mathbb{Z} \quad (2.1)$$

is an orthonormal basis. Wavelet series then can be defined as follows:

$$f(x) = \sum_k \alpha_k \phi_{0k}(x) + \sum_{j=0}^{\infty} \sum_k \beta_{jk} \psi_{jk}(x) \quad (2.2)$$

Where α_k and β_{jk} are approximation and details coefficient respectively. ψ_{jk} , $k \in \mathbb{Z}$ is basis for W_j . The relation in Equation (2.2) is called a multiresolution expansion of f . To turn Equation (2.2) into wavelet expansion we use the following expression

$$\psi_{j,k}(x) = 2^{\frac{j}{2}} \psi(2^j x - k), j, k \in \mathbb{Z} \quad (2.3)$$

Basically the function $\varphi_{j,k}(x)$ and $\psi_{j,k}(x)$ are called the scaling function (father wavelet) and the mother wavelet respectively. In terms of the wavelet coefficients, the wavelet equation [9] is

$$\psi(x) = \sum_k^{N-1} g_k \sqrt{2} \varphi(2x - k) \quad (2.4)$$

Where $g_1, g_2 \dots g_{N-1}$ are high pass wavelet coefficients. Writing the scaling equation in terms of the scaling coefficients as given below yields

$$\varphi(x) = \sum_k^{N-1} h_k \sqrt{2} \varphi(2x - k) \quad (2.5)$$

The function $\varphi(x)$ is the scaling function and the coefficients $h_0, h_1 \dots h_{N-1}$ are low pass filter scaling coefficients. The wavelet and scaling coefficients are related by the quadrature mirror relationship, which is

$$g_n = (-1)^n h_{1-n+N} \quad (2.6)$$

The term N is the number of vanishing moment [9].

2.2 Wavelet Family

There are a number of basis functions that can be used as the mother wavelet for Wavelet Transformation. Since the mother wavelet produces all wavelet functions used in the through translation and scaling, it determines the characteristics of the resulting Wavelet Transform. Therefore, the details of the particular application should be taken into account and the appropriate mother wavelet should be chosen in order to use the Wavelet Transform effectively [1]. Figure below shows among the popular wavelets that are used nowadays.

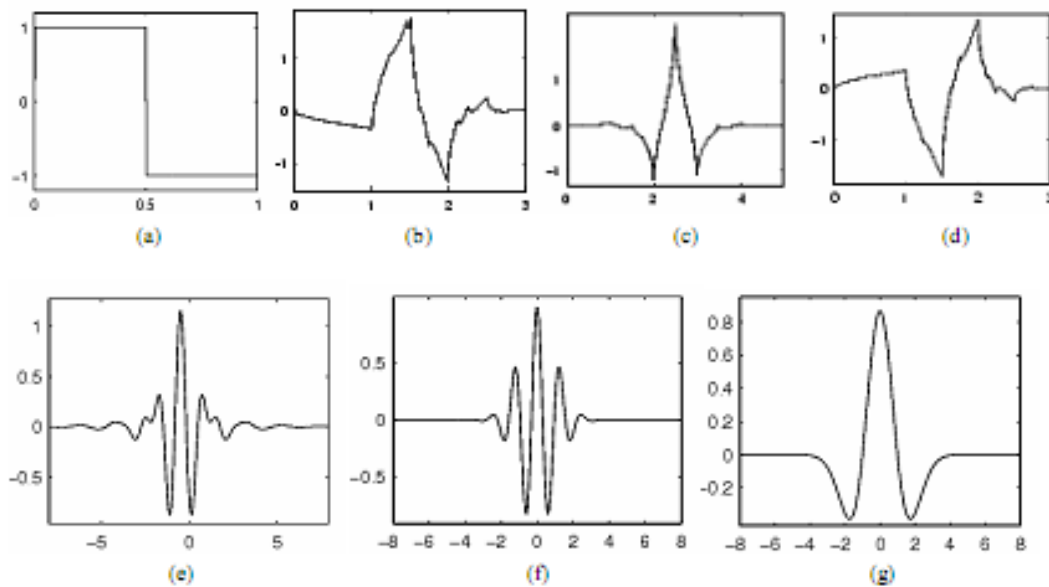


Figure 1: Wavelet families (a) Haar (b) Daubechies4 (c) Coiflet1 (d) Symlet2 (e)Meyer (f) Morlet (g) Mexican Hat

2.3. Discrete Wavelet Transform

Calculating wavelet coefficient at every possible scale generates a lot of data. DWT is wavelet transform scheme using filter and was developed in 1988 by Mallat [10]. This very practical filtering algorithm yields a fast wavelet transform, a box into which signal passes and out by separating the signal into its low pass and high pass components. As stated in the first section of this chapter, the approximations and details coefficients are essential in data denoising. For many signals, the low-frequency content is the most important part. It is what gives the signal its identity. The high-frequency content, on the other hand, imparts flavor or nuance [11]. For example, the human voice, if high frequency component is removed the voice sound is different, in contrast if low frequency component is removed the voice expected to have gibberish sound. The approximations are the high-scale, low-frequency components of the signal. The details are the low-scale, high-frequency components [11]. The noise coefficients that also occur when DWT is performed can be eliminated by applying certain threshold value on the high frequency coefficients or the details coefficients; this is basically the idea of

denoising using threshold method. The DWT of data follows a certain algorithm; this can be summarized as follows [11]:

- 1) Given a signal s of length N , the DWT consists of $\log_2 N$ stages at most. Starting from S , the first step produces two sets of coefficients: approximation coefficients cA_1 , and detail coefficients cD_1 . These vectors are obtained by convolving s with the low-pass filter Lo_D for approximation, and with the high-pass filter Hi_D for detail, followed by dyadic decimation [11].
- 2) The next step splits the approximation coefficients cA_1 in two parts using the same scheme, replacing s by cA_1 and producing cA_2 and cD_2 , and so on [11].

2.3.1 One Dimensional data (Signal)

Using algorithm that is discussed in the previous section, the decomposition of one dimensional data can be simplified as in Figure 2.

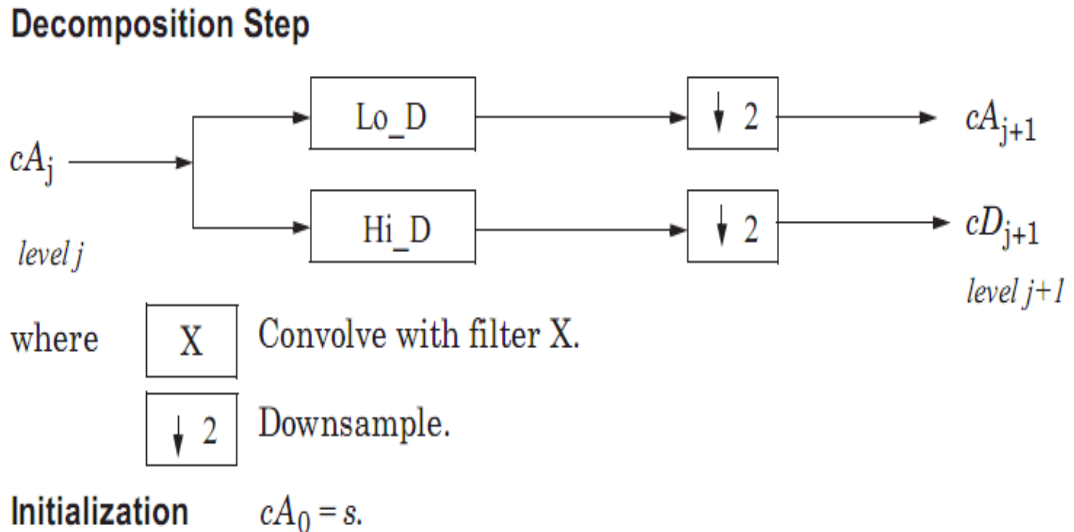


Figure 2 : Decomposition of One Dimensional data [11]

For decomposition of the signal at level 3 for example, the resulting structure is shown in the Figure 3.

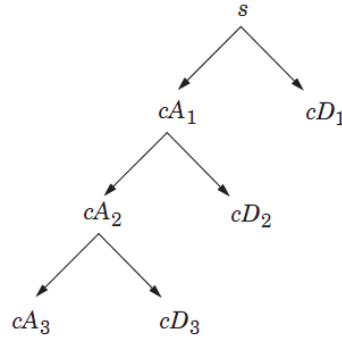


Figure 3 : Mallat's decomposition tree [11]

Conversely starting from cA_j and cD_j , the inverse Discrete Wavelet Transform (IDWT) reconstruct cA_{j-1} , inverting the decomposition step by inserting zeros and convolving the results with the reconstruction filters. The reconstruction process can be described as shown in the Figure 4.

Reconstruction Step

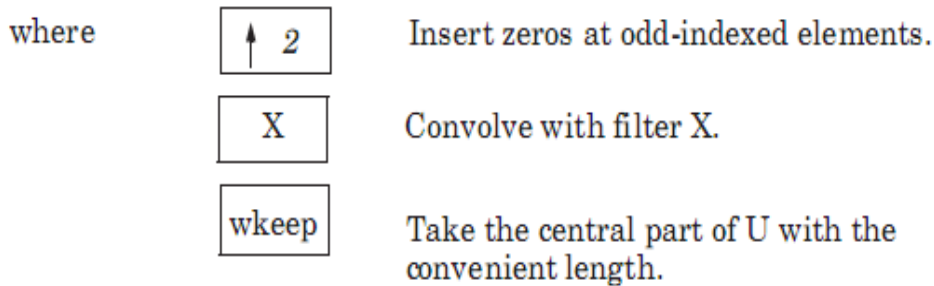
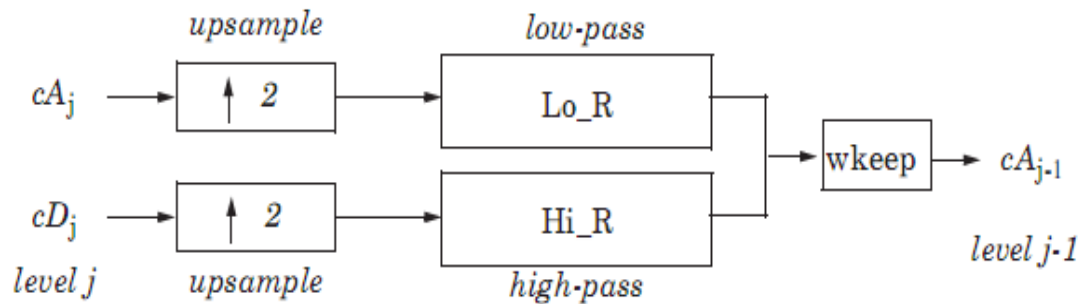
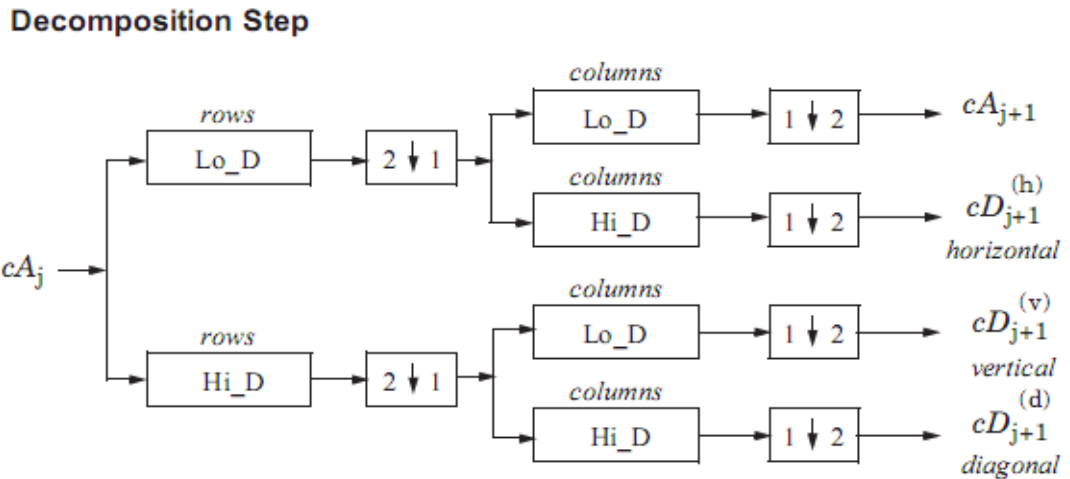


Figure 4 : Reconstruction of One Dimensional data [11]

As shown in the Figure 4 above, the original signal is passes through two complementary filters and emerges as two signals. The low pass filter function is defined by equation (2.4) while the high pass filter function is defined by equation (2.5). If the two produced signals are added, the total number of the added signal will be double of the original signal [11]. This will complicate the wavelet transformation because the size of the data is increased. To overcome this problem, downsampling is introduced [11]. By looking carefully at the computation, we may keep only one point out of two in each of the two N-length samples to get the complete information. This is the notion of downsampling. We produce two sequences called cA and cD [11].

2.3.2 Two Dimensional data

For images, a similar algorithm is possible for two-dimensional wavelets and scaling functions obtained from one-dimensional wavelets by tensorial product. This kind of two-dimensional DWT leads to a decomposition of approximation coefficients at level j in four components: the approximation at level $j + 1$ and the details in three orientations (horizontal, vertical, and diagonal). The following charts describe the basic decomposition and reconstruction steps for images. The new details coefficients are introduced for the image DWT, there are include horizontal, vertical and diagonal [11].



where

$\begin{matrix} \boxed{2 \downarrow 1} \end{matrix}$	Downsample columns: keep the even indexed columns.
$\begin{matrix} \boxed{1 \downarrow 2} \end{matrix}$	Downsample rows: keep the even indexed rows.
$\begin{matrix} \text{rows} \\ \boxed{X} \end{matrix}$	Convolve with filter X the rows of the entry.
$\begin{matrix} \text{columns} \\ \boxed{X} \end{matrix}$	Convolve with filter X the columns of the entry.

Initialization $CA_0 = s$ for the decomposition initialization.

Figure 5 : Decomposition of 2-Dimensional data (Image) [11]

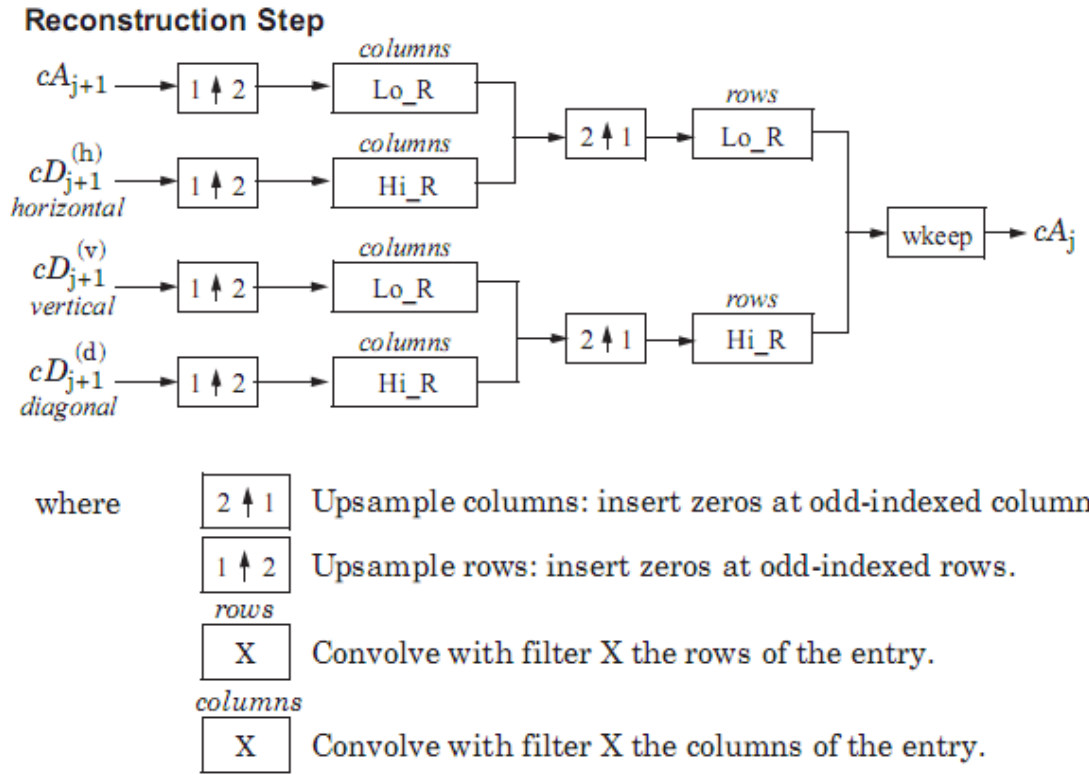


Figure 6: Reconstruction of 2-Dimensional data [11]

The reconstruction image can be described from the Figure 6. As for two level of DWT, the two dimensional wavelet trees have the form of:

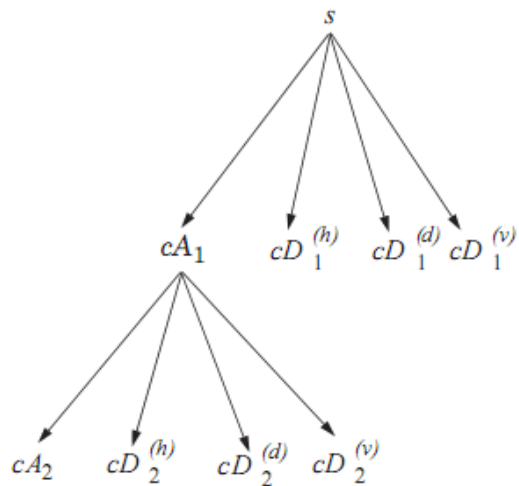


Figure 7 : Two level of Mallat's Decomposition Trees (Image) [11]

HH3	HH3	HH2	LH1
HH3	HH3		
HH2		HH2	
HL1			HH1

Figure 8 : Three level of Mallat's Decomposition Trees (Image)

2.4 Denoising Method

Donoho and Johnstone [10] pioneered the work on filtering of additive Gaussian noise using wavelet thresholding. From their properties and behavior, wavelets play a major role in image compression and image denoising. Since our topic of interest is data denoising, the latter application is discussed in detail. Wavelet coefficients calculated by a wavelet transform represent change in the time series at a particular resolution. By considering the time series at various resolutions, it is then possible to filter out noise.

The term wavelet thresholding is explained as decomposition of the data or the image into wavelet coefficients, comparing the detail coefficients with a given threshold value, and shrinking these coefficients close to zero to take away the effect of noise in the data [12]. The image is reconstructed from the modified coefficients. This process is also known as the inverse discrete wavelet transform. During thresholding, a wavelet coefficient is compared with a given threshold and is set to zero if its magnitude is less than the threshold; otherwise, it is retained or modified depending on the threshold rule.

Thresholding distinguishes between the coefficients due to noise and the ones consisting of important signal information. The choice of a threshold is an important point of interest. There exist various methods for wavelet thresholding, which rely on the choice of a threshold value. Some typically used methods for data noise removal include VisuShrink, SureShrink and BayesShrink [14, 13, 10]. Prior to the discussion of these methods, it is necessary to know about the two general categories of thresholding. They are hard thresholding and soft thresholding types [12].

2.4.1 Hard Thresholding

The hard-thresholding can be defined as [10]

$$T_H = \begin{cases} 0, & \text{in all other regions} \\ x, & |x| \geq t \end{cases} \quad (2.7)$$

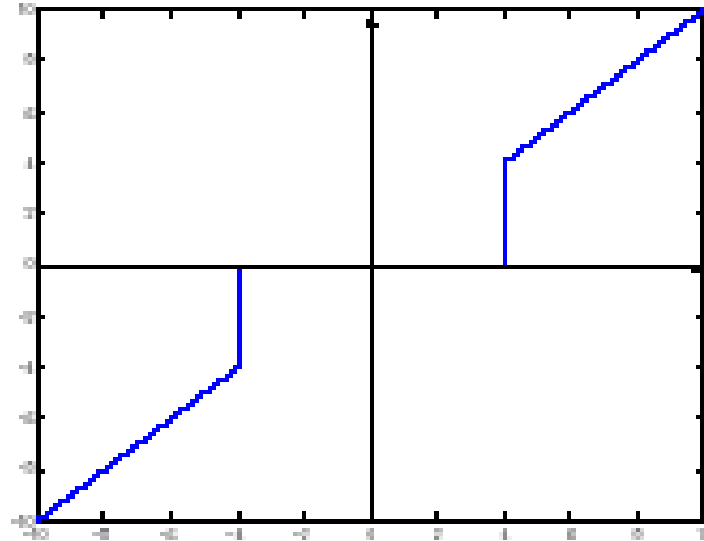


Figure 9 : Hard Thresholding

Thus, all coefficients whose magnitude is greater than the selected threshold value remain as they are and the others with magnitudes smaller than t are set to zero.

zero. It creates a region around zero where the coefficients are considered negligible [12].

2.4.2 Soft Thresholding

Soft thresholding is where the coefficients with greater than the threshold are shrunk towards zero after comparing them to threshold value. It is defined as follows [10]

$$T_H = \begin{cases} 0, & \text{in all other regions} \\ \text{sign}(x)(|x| - t), & |x| > t \end{cases} \quad (2.8)$$

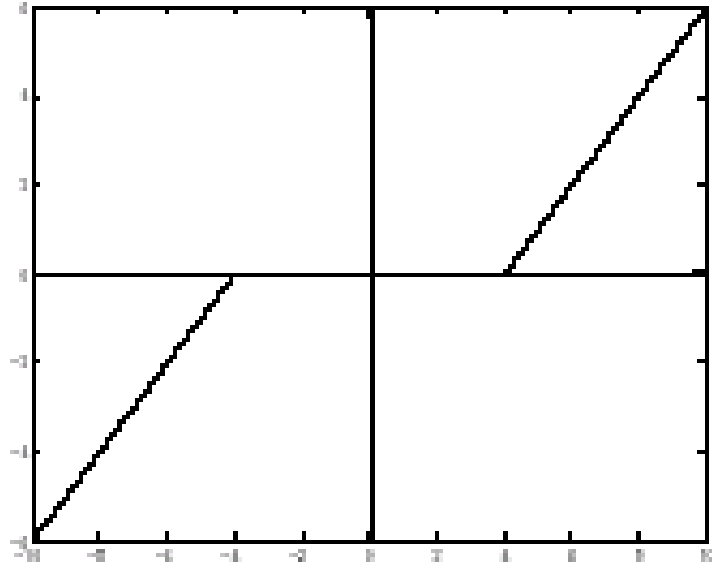


Figure 10 : Soft Thresholding

2.4.2 VisuShrink

Visushrink is thresholding by applying the Universal threshold proposed by Donoho and Johnstone. This threshold is given by [10]

$$t = \sigma \sqrt{2 \log n} \quad (2.9)$$

σ^2 is the noise variance present in the signal and n represents the signal size or number of samples. An estimate of the noise level σ was defined based on the median absolute deviation [donoho] given by [3]

$$\hat{\sigma} = \frac{\text{median} (\{g_{j-1,k} | :k=0,1,\dots,2^{j-1}-1\})}{0.6745} \quad (2.10)$$

Where $g_{j-1,k}$ corresponds to the detail coefficients in the wavelet transform. Universal threshold was used in image denoising and application denoising only.

2.4.3 Rigrsure

‘Rigrsure’ uses for the soft threshold estimator a threshold selection rule based on the Stein’s Unbiased Estimate of Risk (quadratic loss function). One gets an estimate of the risk for a particular threshold value t . Minimizing the risk in t gives a selection the threshold value [11]. This method to find threshold value t was applied in signal denoising only.

2.4.4 Heursure

‘Heursure’ is a mixture of the two previous options. As a result, if the signal to noise ratio is very small, the SURE estimate is very noisy. If such a situation is detected, the fixed from threshold is used [11]. This method to find threshold value t was applied in signal denoising only.

2.5 Noise

Noise is undesired information that contaminates any signals or image. Typical data(s) are contaminated with noise modeled with either a Gaussian, uniform, or salt or pepper distribution. For this thesis there are three types of noises that are used i.e Gaussian White Noise, Salt and Pepper and Speckle. Noise is present in image either in an additive or multiplicative form [4].

An additive noise follows the rule [15]

$$w(x, y) = s(x, y) + n(x, y) \quad (2.11)$$

While the multiplicative noise as follow [15]

$$w(x, y) = s(x, y) \times n(x, y) \quad (2.12)$$

Where $s(x,y)$ is the original signal, $n(x,y)$ denotes the noise introduced to the signal to produce the corrupted image or signal $w(x, y)$ [15].

2.5.1 Gaussian noise

Gaussian noise is the noise that is used for both tested signal and image in this thesis. This noise is basically the common noise that is applied in data denoising analysis. As the name indicates, this type of noise has a Gaussian distribution, which has a bell shaped probability distribution function given by [12],

$$F(g) = \frac{1}{\sqrt{2\pi\sigma^2}} e^{-(g-m)^2 / 2\sigma^2} \quad (2.13)$$

Where g represents the gray level, m is the mean or average of the function, and σ is the standard deviation of the noise. For the 1-dimensional data, the SNR of Gaussian noise that is added to tested signals is 3dB, meanwhile for two dimensional data, the Gaussian noise with zero mean and variance 0.05 is used.

The Figure 11 below shows the Gaussian white noise with mean zero and variance of 0.05.

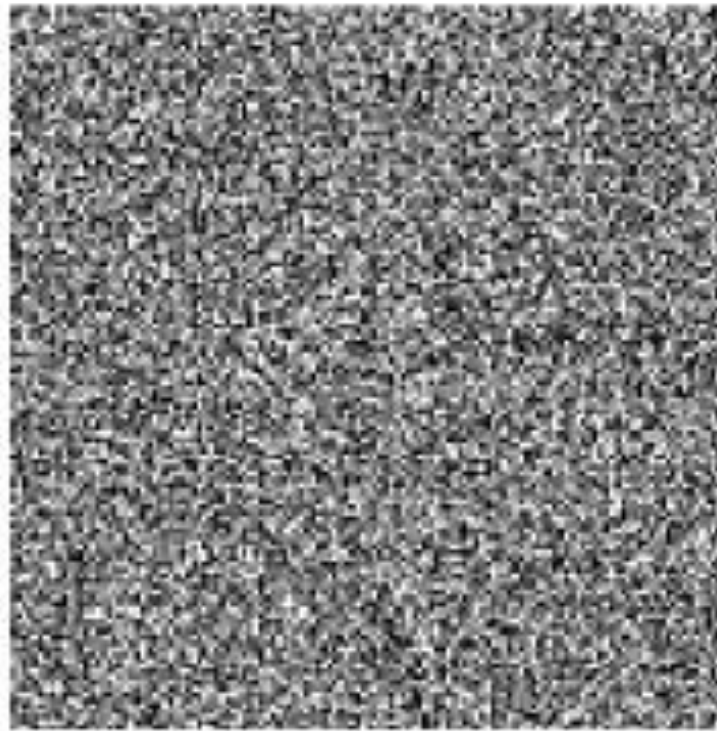


Figure 11 : Gaussian Noise with variance 0.05 [12]

2.5.2 Salt and pepper noise

Salt and pepper noise is an impulse type of noise, which is also referred to as intensity spikes [16]. Generally this is due to errors in data transmission. It has only two possible values, a and b. The probability of each is typically less than 0.1. The corrupted pixels are set alternatively to the minimum or to the maximum value, giving the image a “salt and pepper” like appearance. Unaffected pixels remain unchanged. For an 8-bit image, the typical value for pepper noise is 0 and for salt noise 255. The salt and pepper noise is generally caused by malfunctioning of pixel elements in the camera sensors, faulty memory locations,

or timing errors in the digitization process. Salt and pepper noise with a variance of 0.05 is shown in Figure 12 below. Salt and Pepper noise is used in two dimensional data denoising of this thesis.

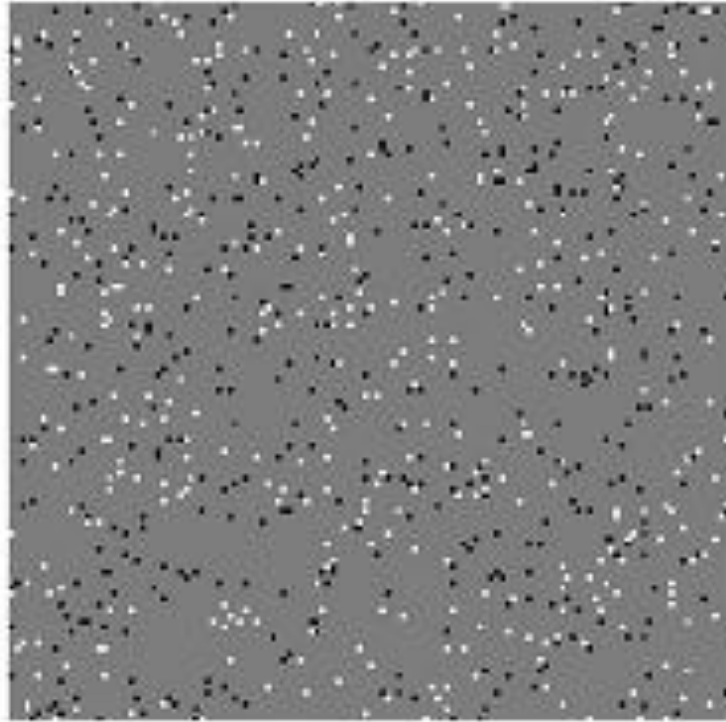


Figure 12 : Speckle Noise with variance 0.05 [12]

2.5.3 Speckle noise

Speckle noise is a multiplicative noise [17]. This type of noise occurs in almost all coherent imaging systems such as laser, acoustics and SAR (Synthetic Aperture Radar) imagery. The source of this noise is attributed to random interference between the coherent returns. Fully developed speckle noise has the characteristic of multiplicative noise. Speckle noise follows a gamma distribution and is given as [12]

$$F(g) = \frac{g^{a-1}}{(a-1)!a^\alpha} e^{-\frac{g}{a}} \quad (2.12)$$

where variance is $a^2\alpha$ and g is the gray level. For two dimensional data, speckle noise with variance 0.05 is used. The speckle noise is shown in Figure 13.

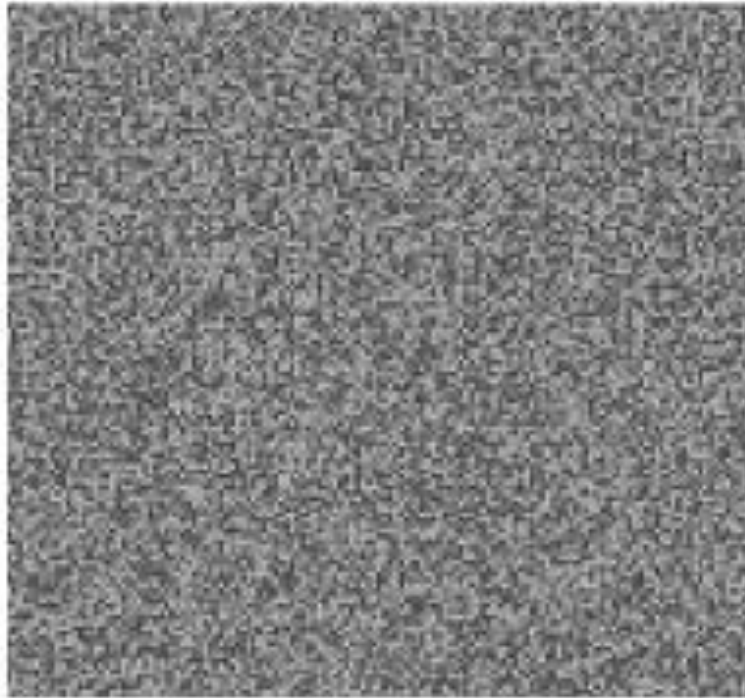


Figure 13 : Speckle noise with 0.05 variance [12]

2.6 Electrocardiography (ECG)

Electrocardiography ECG or EKG [from the German Elektrokardiogramm] is a transthoracic interpretation of the electrical activity of the heart over time captured and externally recorded by skin electrodes. It is a noninvasive recording produced by an electrocardiographic device [18].

The morphology of ECG signal has been used for recognizing much variability's of heart activity, so it is very important to get the parameters of ECG signal clear without noise [19]. This step gives a full picture and detailed information about the electrophysiology of the heart diseases and the ischemic changes that may occur like the myocardial infarction, conduction defects and arrhythmia. In order to support clinical decision-making, reasoning tool to the ECG signal must be clearly represented and filtered, to remove out all noises and artifacts from the signal. ECG signal is one of the biosignals that is considered as a non-stationary signal and needs a hard work to denoising [20, 21]. The typical ECG data is shown in the Figure 14.

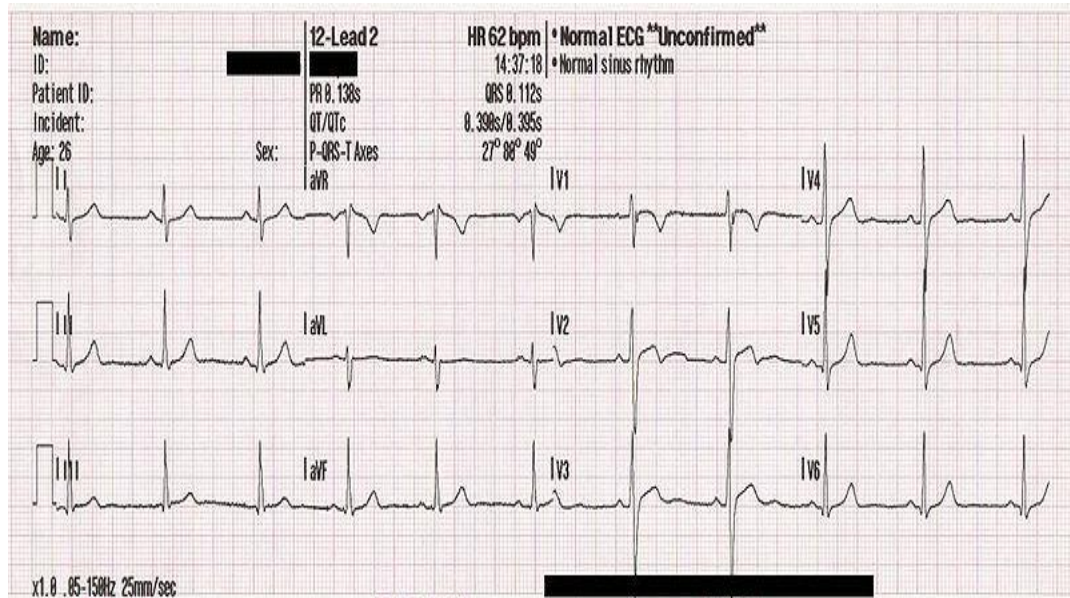


Figure 14 : 12 Lead ECG of a 26-year-old male. [18]

2.7 Comparative study measurement

Comparative study of tested data for both one dimensional and two dimensional are done using Signal to Noise Ratio (SNR), Root Mean Squared

Error (RMSE) and Peak Signal to Noise Ratio (PSNR). These three tools are very important as it is the typical method to measure the performance of wavelet in data denoising.

2.7.1 One-dimensional data

For the one dimensional data, the signal to noise ratio is given by

$$SNR=10\log\frac{\sum x^2}{\sum \bar{x}^2} \quad (2.13)$$

With x is original signal and \bar{x} is the denoised signal

The root mean squared of the signal on the other hand is given by

$$RMSE=\frac{\sqrt{\sum (x-\bar{x})^2}}{N} \quad (2.13)$$

2.7.2 Two-dimensional data

For two dimensional data, the Peak Signal toNoise Ratio is given by

$$PSNR=\frac{10\log 255^2}{mse} \quad (2.14)$$

Where mse is the mean squared error between the original and the denoised image with size $I \times J$. The RMSE is calculated by taking the square root of mse

$$mse=\frac{1}{IxJ}\sum_{i=1}^I\sum_{j=1}^J[x(i,j)-\bar{x}(i,j)]^2 \quad (2.15)$$

CHAPTER 3 METHODOLOGY

3.1 Procedure identification

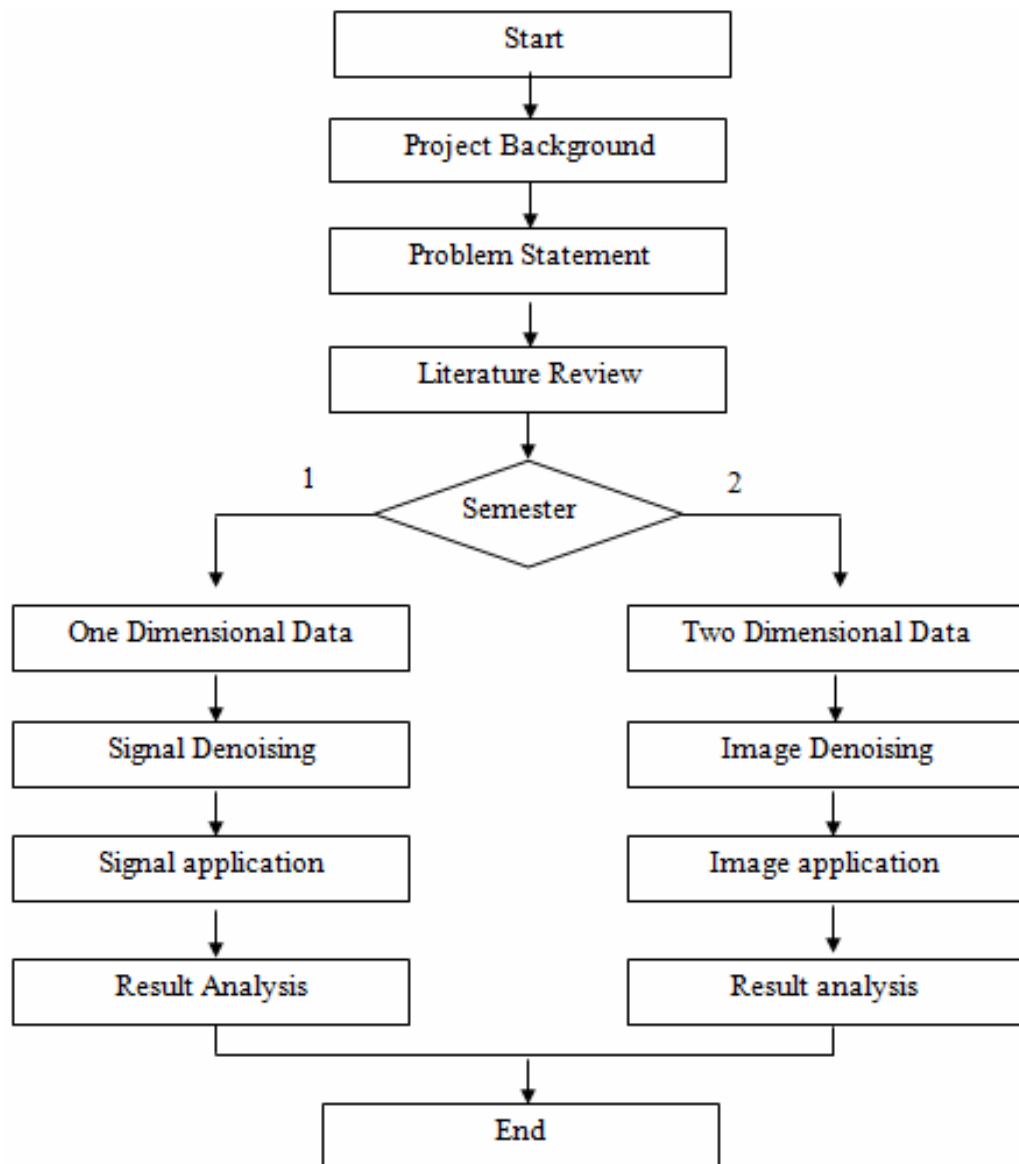


Figure 15 : Flow chart of thesis

3.2 Data

For this project, two types of data were used. First was 1-dimensional data or signal which consisted of three types i.e. blocks, bumps and heavy sine with a fixed length of $N = 1024$. Second was 2-dimensional data or image which consisted of six types i.e Barbara, Mandrill, Airplane, Bridge, Couple and Sailboat with a fixed resolution of 512×512 . The figures of these tested data are shown in Appendix A. These two types of data is a standardized data that is commonly used in data denoising field. Apart from these two, there also application data used to show that denoising is applicable and useful in real life. This application data used were Kuala Lumpur Composite Index (KLCI) data and Electrocardiography (ECG) data.

3.3 Denoising

3.3.1 Signal Denoising

The overall procedure for signal denoising can be described from Figure 18 below.

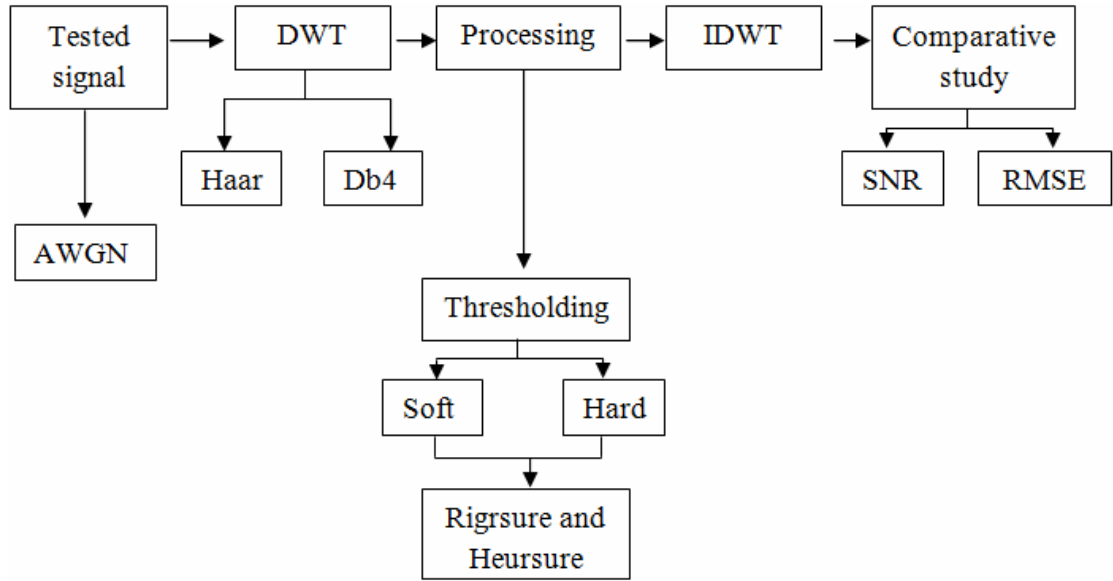


Figure 16 : Flow chart of signal denoising

Firstly, the tested signal was added with 3dB White Gaussian Noise before being transformed using discrete wavelet transform (DWT) using both Haar and Daubechies4 wavelet basis functions. Then, the coefficients of DWT were processed or manipulated using thresholding method to remove the noise. Next, IDWT was performed on the coefficients and lastly, Signal to Noise Ratio (SNR) and Root Mean Square Error (RMSE) were calculated in order to compare the results. This procedure was also applied to real data except that the real data was not being added with AWGN because it was already corrupted with noise and the thresholding method used was only global thresholding.

3.3.2 Image denoising.

The overall procedure for image denoising is described in Figure 17 below.

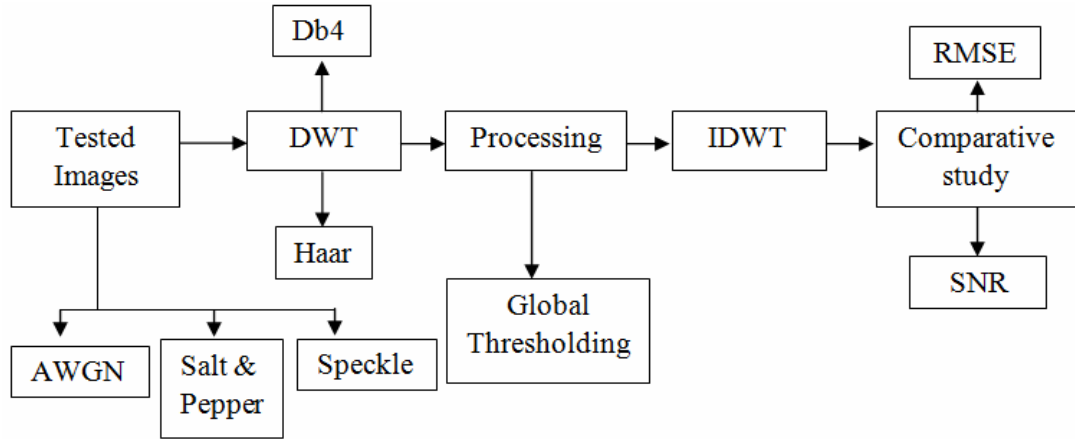


Figure 17 : Flow chart of image denoising

For 2-dimensional data, the tested images were corrupted with three types of noise; Additive White Gaussian Noise (AWGN), Salt and Pepper noise and Speckle noise. The same basis functions, Haar and Daubechies4 were used in transforming the tested images using DWT. For image denoising, universal thresholding was used instead of Rigrsure and Heursure. The threshold value t is then applied globally to all details coefficients (horizontal,vertical and diagonal). After the coefficients were thresholded, the image was then reconstructed using IDWT. Lastly, comparative study was done using PSNR and RMSE. The same procedure was applied to real data using Electrocardiography (ECG).

3.4 Tools

The software used in this project was MATLAB 7.1

CHAPTER 4

RESULT AND DISCUSSION

4.1 Results

4.1.1 Signal denoising

The values of SNR and RMSE for the three tested signals are tabulated in Table 1 to Table 4 below. These tabulated data were used to determine the optimum level and the best wavelet function for denoising as stated in the objectives. For signal denoising, the wavelet transform was done up to 10 levels. The yellow box indicates the optimum level for the wavelet, while the green box indicates the lowest RMSE of DWT. The optimum level of DWT can be determined when the value of SNR slowly becomes constant. The overall optimum level of denoising is given in Table 5 and the overall wavelet performance is given in Table 11. Further discussion can be found in Section 4.2.

Table 1: Haar Wavelet Soft Thresholding

Level		1	2	3	4	5	6	7	8	9	10
Blocks	Heursure	SNR 15.6547	17.1414	18.3061	18.4991	18.6357	18.7287	18.7288	18.5099	18.3827	18.3827
		RMSE 0.7415	0.6248	0.5464	0.5344	0.5261	0.5205	0.5205	0.5337	0.5416	0.5416
	Rigsure	SNR 15.8290	17.9597	19.4106	19.6612	19.8405	19.9637	19.9639	19.4897	14.6713	9.2621
		RMSE 0.7267	0.5687	0.4812	0.4675	0.4570	0.4515	0.4515	0.4768	0.8304	1.5478
Bumps	Heursure	SNR 13.6489	14.9072	15.5966	15.8632	15.9281	15.9631	15.9638	15.8590	15.7453	15.7453
		RMSE 0.7284	0.6302	0.5821	0.5645	0.5603	0.5581	0.5580	0.5648	0.5722	0.5722
	Rigsure	SNR 13.6472	15.3644	16.1375	16.4408	16.5150	16.5551	16.5559	11.4729	11.0876	8.9959
		RMSE 0.7280	0.5970	0.5470	0.5282	0.5237	0.5213	0.5212	0.9358	0.9783	1.2477
Heavy Sine	Heursure	SNR 12.8223	15.5294	18.1324	19.1493	19.2261	18.9807	18.1582	18.1673	18.2577	18.2577
		RMSE 0.7120	0.5214	0.3864	0.3437	0.3487	0.3504	0.3852	0.3848	0.3808	0.3808
	Rigsure	SNR 12.8207	15.4989	17.8680	18.9241	18.9969	18.7638	11.8828	11.8850	4.5124	4.5162
		RMSE 0.7122	0.5232	0.3983	0.3527	0.3498	0.3593	0.7934	0.7932	1.8535	1.8527

Optimum level	
Lowest RMSE	

Table 2: Haar Wavelet Hard Thresholding

Level		1	2	3	4	5	6	7	8	9	10
		SNR	RMSE	SNR	RMSE	SNR	RMSE	SNR	RMSE	SNR	RMSE
Blocks	Heursure	15.7995	17.9914	18.4129	18.8894	18.8957	18.9090	18.9101	18.9101	18.9101	18.9101
		0.7323	0.5846	0.5587	0.5309	0.5305	0.5298	0.5297	0.5344	0.7162	1.4897
	Rigsure	15.7632	17.7189	18.1136	18.5567	18.5625	18.5748	18.5758	18.5048	15.9557	9.5945
		0.1097	0.0607	0.0547	0.0483	0.0482	0.0482	0.0482	0.0482	0.0482	0.0482
Bumps	Heursure	13.6489	14.9265	15.0096	15.0646	15.0659	15.0657	15.0659	15.0659	15.0659	15.0659
		0.7284	0.6288	0.6228	0.6189	0.6188	0.6188	0.6188	0.6188	0.6188	0.6188
	Rigsure	13.5747	13.9424	14.0085	14.0522	14.0532	14.0530	14.0532	13.0062	12.7368	9.9389
		0.7182	0.5317	0.4616	0.4407	0.4384	0.4355	0.4456	0.4470	0.4470	0.4664
Heavy	Heursure	12.8223	15.3167	17.7526	18.6747	18.6783	18.4962	18.4962	18.4952	18.4952	18.4952
		0.7120	0.5343	0.4036	0.3630	0.3628	0.3705	0.3705	0.3706	0.3706	0.3706
Sine	Rigsure	12.7446	14.9837	15.5785	15.9667	15.9686	15.8701	15.2398	15.2393	7.5602	7.5679
		0.7184	0.5552	0.5184	0.4958	0.4957	0.5013	0.5391	0.5391	1.3050	1.3038

Optimum level	
Lowest RMSE	

Table 3: Db4 Wavelet Soft Thresholding

Level		1	2	3	4	5	6	7	8	9	10	
Blocks	Heursure	SNR	15.4420	16.9445	16.9687	17.1951	17.2264	17.2938	17.2320	17.0458	17.0578	17.0481
		RMSE	0.7592	0.6015	0.5385	0.5286	0.5286	0.5286	0.5288	0.5288	0.5284	0.5284
	Rigrsure	SNR	15.5786	17.7726	18.6842	19.0248	19.0725	19.1761	19.0811	18.7993	18.8172	18.5547
		RMSE	0.7818	0.7086	0.6616	0.6536	0.6531	0.6531	0.6537	0.6534	0.6534	0.6541
Bumps	Heursure	SNR	13.7912	16.4488	17.6978	18.1102	18.1553	18.2145	18.0110	17.9827	17.9829	17.8710
		RMSE	0.7166	0.5277	0.4570	0.4358	0.4336	0.4306	0.4408	0.4423	0.4423	0.4480
	Rigrsure	SNR	13.7718	16.3835	17.6109	18.0148	18.0589	18.1168	17.9177	17.8900	17.8902	17.5209
		RMSE	0.7182	0.5317	0.4616	0.4407	0.4384	0.4355	0.4456	0.4470	0.4470	0.4664
Heavy	Heursure	SNR	12.7696	15.8344	18.2727	20.2460	21.5006	21.5575	21.6283	21.7128	21.6571	21.6452
		RMSE	0.7164	0.5034	0.3802	0.3029	0.2622	0.2605	0.2583	0.2558	0.2575	0.2578
Sine	Rigrsure	SNR	12.7452	15.7340	18.0379	19.9105	21.1741	21.2286	21.2963	21.3756	20.0382	19.9333
		RMSE	0.7184	0.5092	0.3906	0.3148	0.2722	0.2705	0.2684	0.2660	0.3102	0.3140
Optimum level												
Lowest RMSE												

Table 4: Db4 Wavelet Hard Thresholding

	Level												
	1	2	3	4	5	6	7	8	9	10			
Blocks	Heursure		SNR	15.4493	17.4715	18.4326	18.5938	18.6031	18.5944	18.5910	18.5966	18.5980	18.5980
	RMSE		0.7592	0.6015	0.5385	0.5286	0.5286	0.5286	0.5286	0.5288	0.5284	0.5284	0.5284
	Rigrsure		SNR	15.1942	16.0490	16.6444	16.7506	16.7567	16.7510	16.7487	16.7524	16.7533	16.7433
	RMSE		0.7818	0.7086	0.6616	0.6536	0.6531	0.6536	0.6537	0.6537	0.6534	0.6534	0.6541
Bumps	Heursure		SNR	13.7912	16.4488	16.8206	16.9611	16.9641	16.9723	16.9684	16.9756	16.9737	16.9737
	RMSE		0.7166	0.5277	0.5056	0.4975	0.4973	0.4969	0.4971	0.4967	0.4967	0.4968	0.4968
	Rigrsure		SNR	13.3114	14.8992	15.1561	15.2514	15.2534	15.2589	15.2563	15.2611	15.2599	15.2596
	RMSE		0.7573	0.6308	0.6124	0.6057	0.6056	0.6052	0.6054	0.6054	0.6050	0.6051	0.6052
Heavy Sine	Heursure		SNR	12.7696	15.8344	18.2727	19.9620	21.2377	21.1553	21.1381	21.1328	21.1328	21.0998
	RMSE		0.7164	0.5034	0.3802	0.3130	0.2702	0.2728	0.2735	0.2735	0.2735	0.2735	0.2746
	Rigrsure		SNR	12.2090	14.0145	15.0620	15.5993	15.6536	15.6307	15.6258	15.6243	15.5933	15.5827
	RMSE		0.7641	0.6207	0.5502	0.5172	0.5140	0.5153	0.5156	0.5156	0.5157	0.5176	0.5182
Optimum level													
Lowest RMSE													

The overall value of SNR and RMSE at optimum level are tabulated in the table 5 below.

Table 5: Overall SNR and RMSE at optimum level

		Soft Thresholding				Hard Thresholding			
		Haar		Db4		Haar		Db4	
		SNR	RMSE	SNR	RMSE	SNR	RMSE	SNR	RMSE
Blocks	Heursure	18.3827	0.5205	17.0458	0.5284	18.9101	0.5297	18.5966	0.5284
	Rigrsure	19.9637	0.4515	18.7993	0.6531	18.5758	0.0482	16.7524	0.6534
Bumps	Heursure	15.7453	0.558	17.9827	0.4306	15.0659	0.6188	16.9756	0.4967
	Rigrsure	16.5551	0.5212	17.8900	0.4355	14.0530	0.4355	15.2611	0.6050
Heavy	Heursure	18.2577	0.3437	21.6571	0.2558	18.4952	0.3628	21.1328	0.2702
Sine	Rigrsure	4.5124	0.3498	21.3756	0.2660	15.2398	0.4957	15.6258	0.5153

To further illustrate the optimum level of the two wavelets. Graph of SNR versus level is plotted. As we can see, the optimum level of wavelet transform can be determined when the reading of SNR is constant.

Block Signals

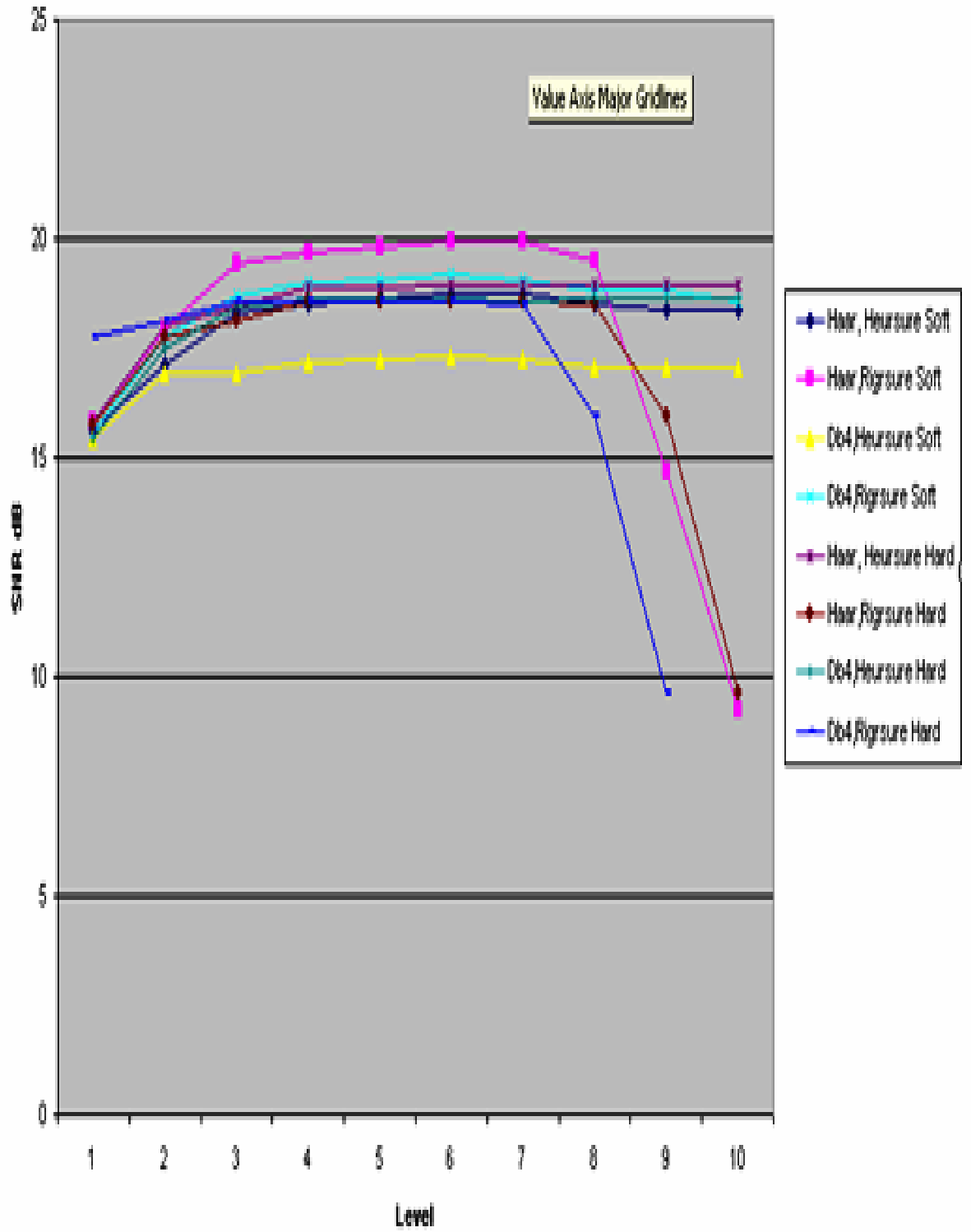


Figure 18 : SNR vs. level for blocks signal

Bumps Signal

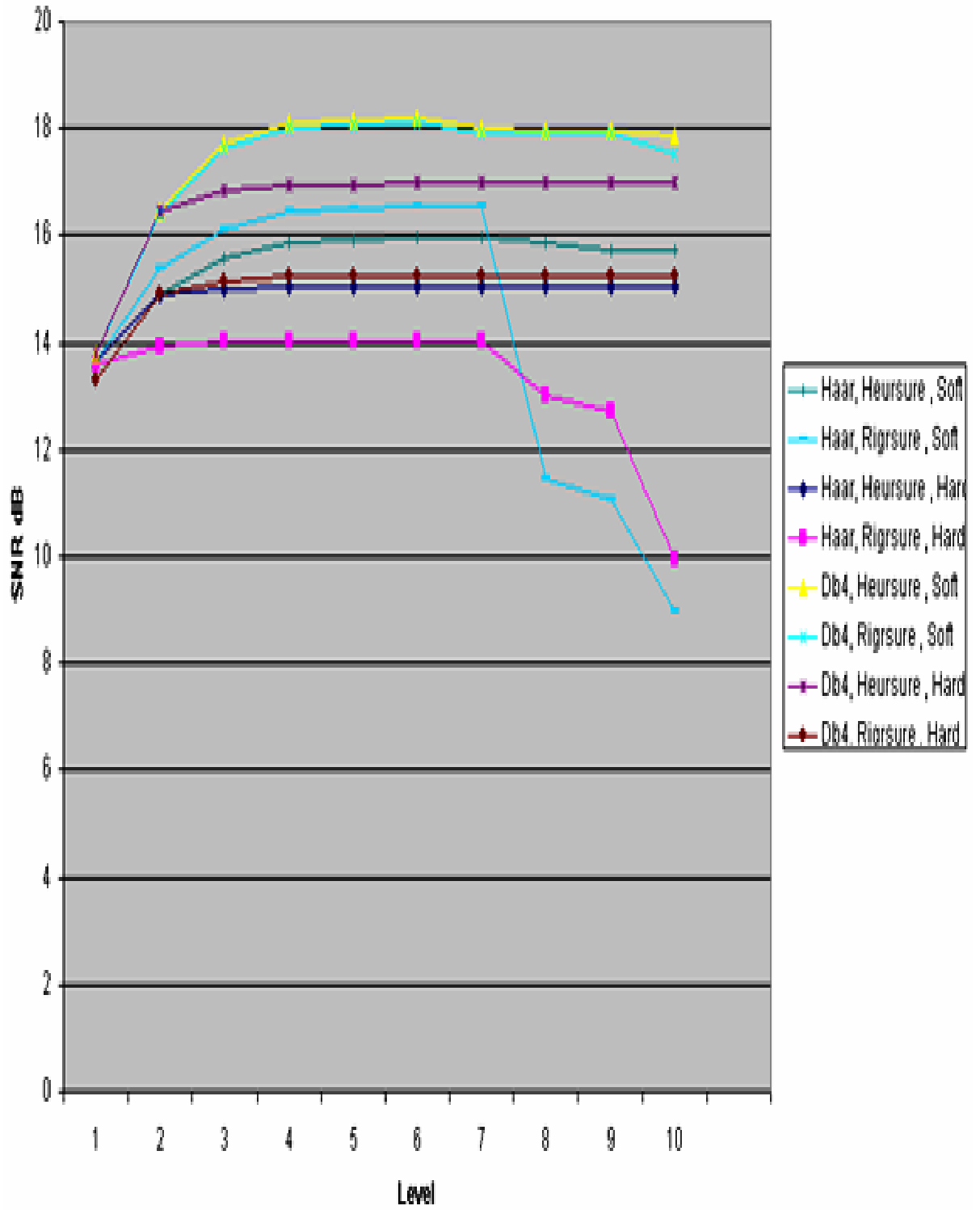


Figure 19 : SNR vs. level for bumps signal

Heavy Sine Signal

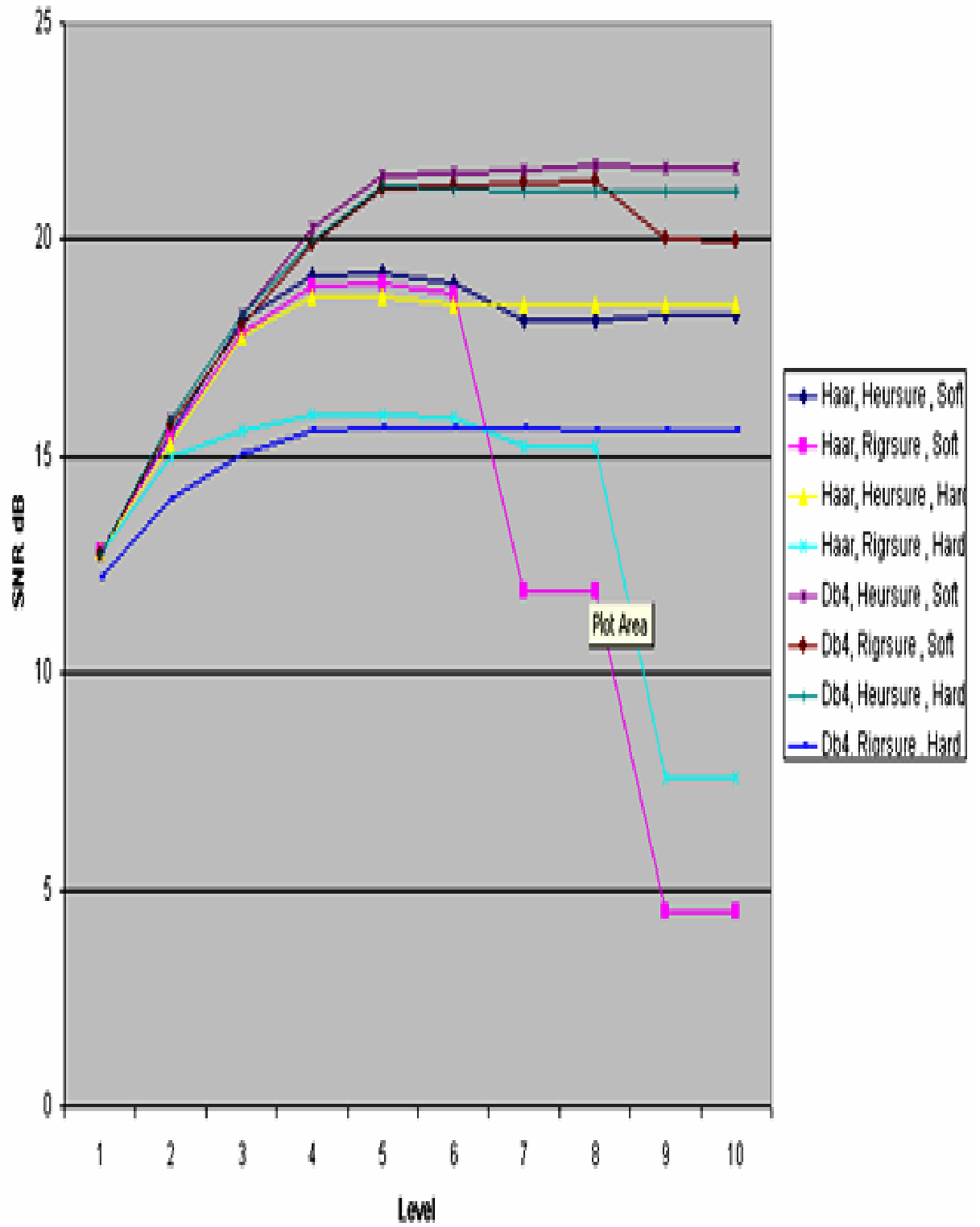


Figure 20 : SNR vs. level for heavy sine signal

As described in Chapter 3, signal denoising consists of adding noise to the original signal, thresholding the signal and reconstructing the signal. This procedure is illustrated in the denoising diagrams from Figure 21 to Figure 28. The breakdown of the denoising diagram is as follows:

- i. The first signal is the original signal or the tested signal
- ii. The second signal is the noisy version of the original signal
- iii. The third signal is the detailed coefficients that were manipulated to remove the noise
- iv. The last signal is the reconstructed signal from the wavelet coefficients

The denoising diagrams below are the wavelet transform at the optimum level for both Haar and Db4 wavelets. As observed from Table 1 to Table 4, the optimum level of Haar wavelet is at 10, while the optimum level of Db4 wavelet is at 8

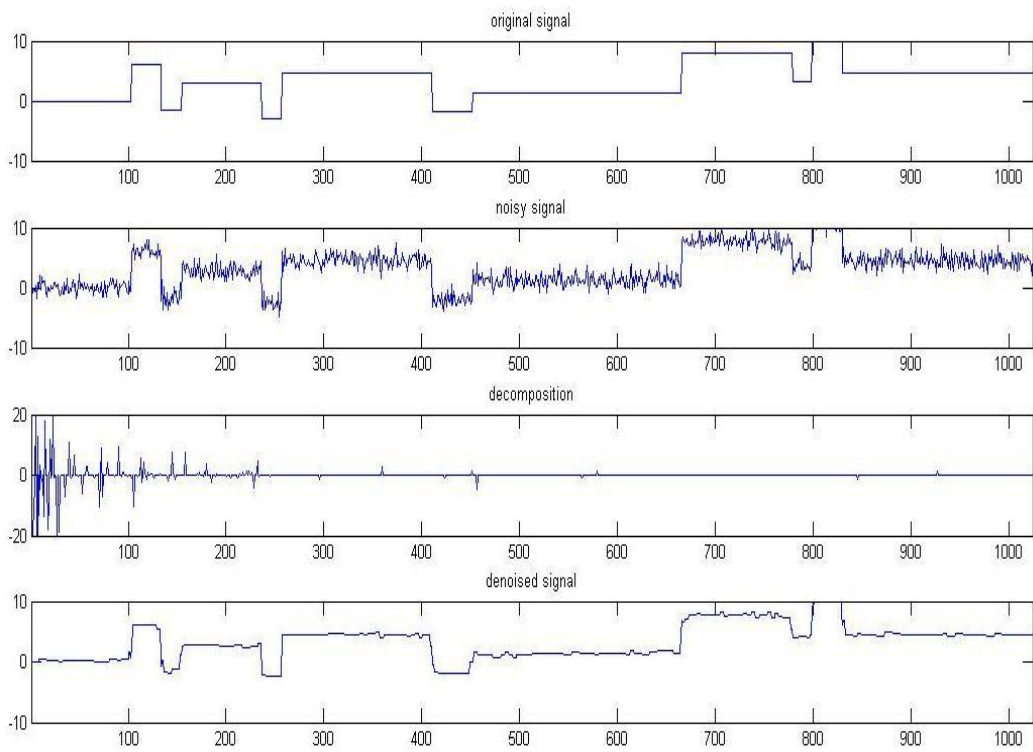


Figure 21: Haar wavelet transform at level 10 using Soft thresholding Rigrsure

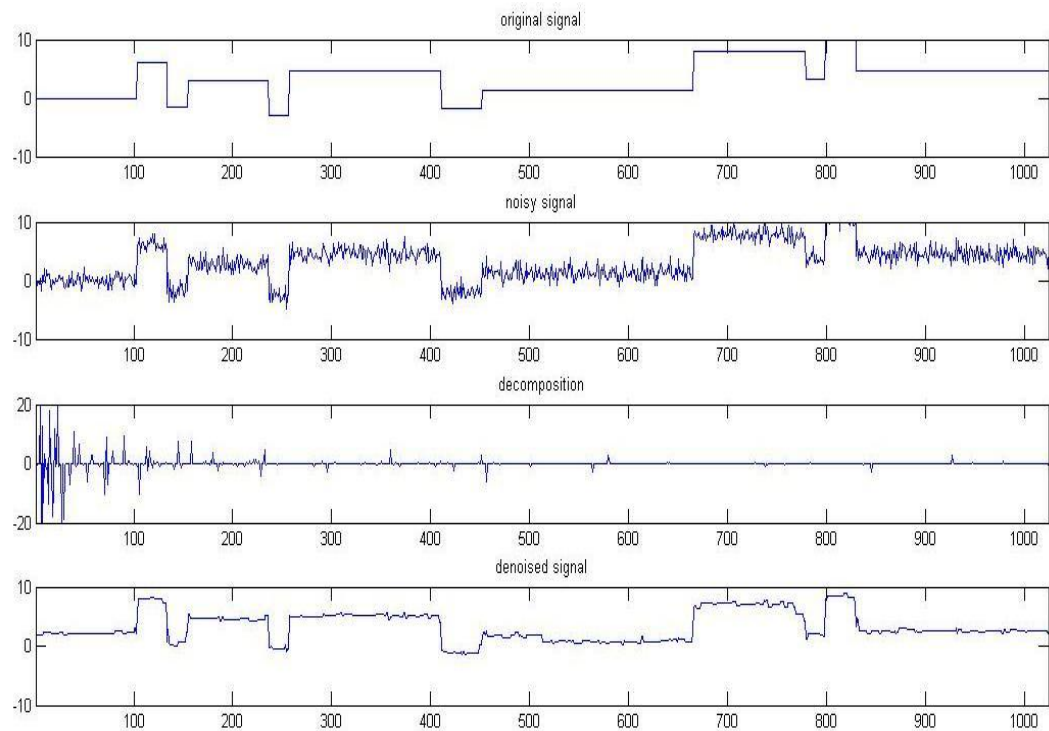


Figure 22 Haar wavelet transform at level 10 using Soft Thresholding Heursure

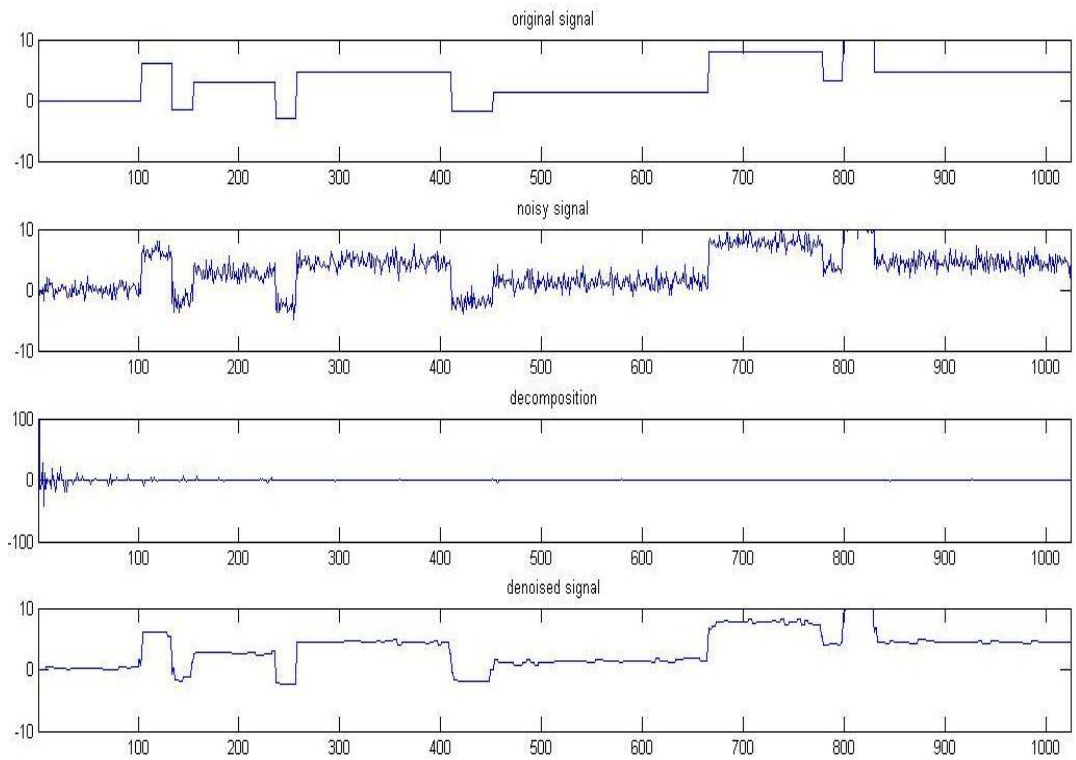


Figure 23 : Haar wavelet transform at level 10 using Hard Thresholding Heursure

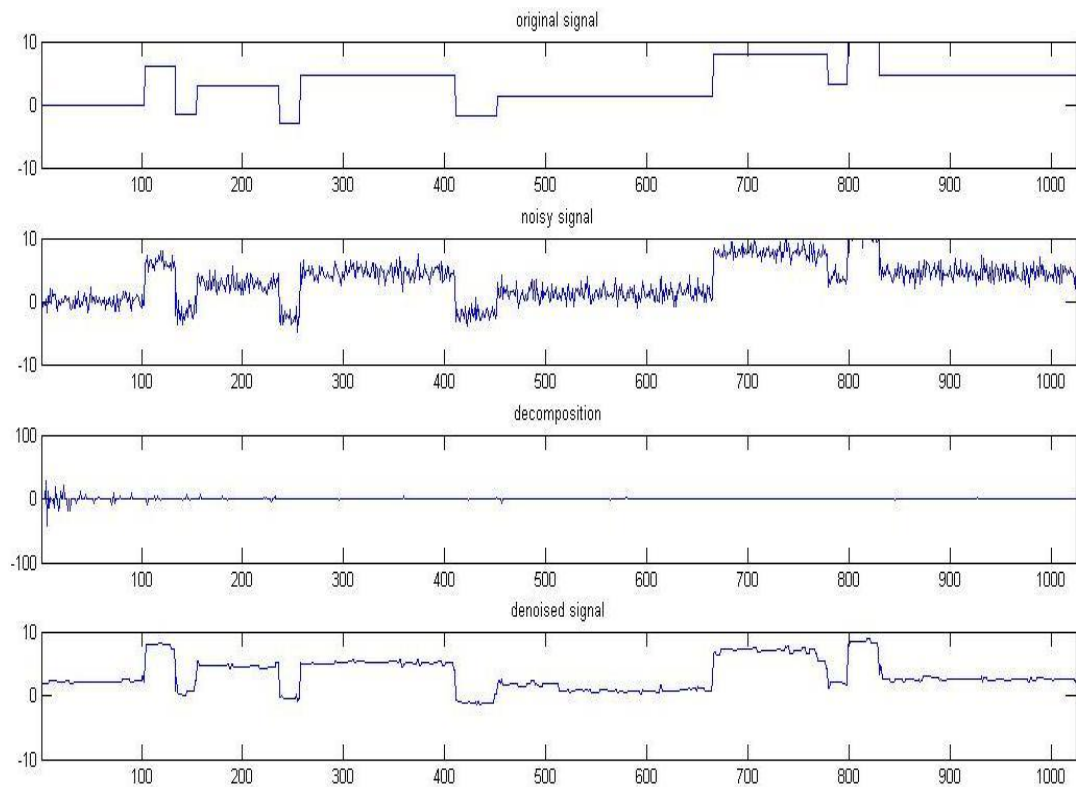


Figure 24 : Haar wavelet transform at level 10 using Hard Thresholding Rigrsure

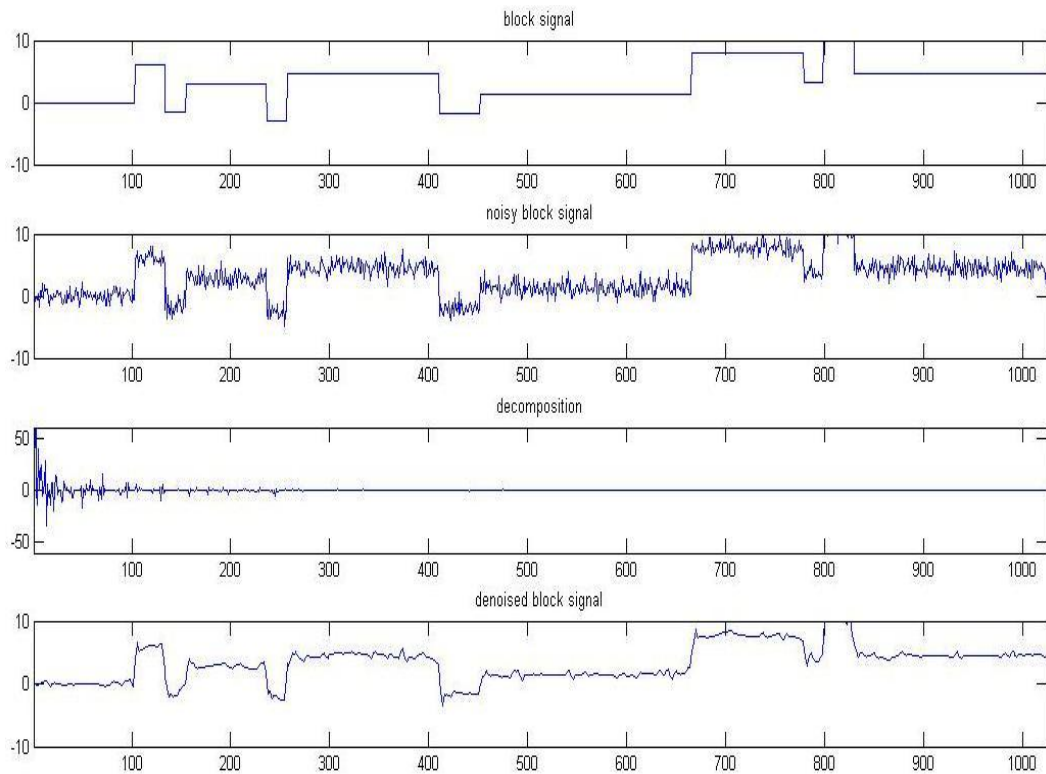


Figure 25 : Db4 wavelet tranform at level 8 using soft thresholding, Heusure

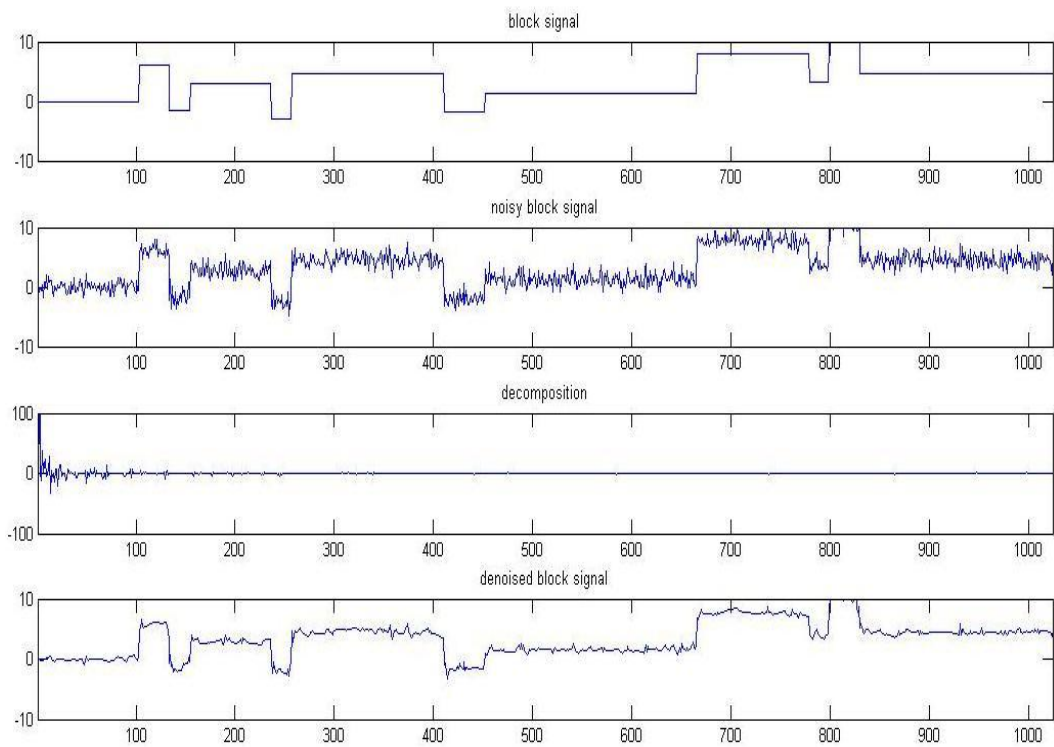


Figure 26 : Db4 wavelet transform at level 8 using soft thresholding, Rigrsure

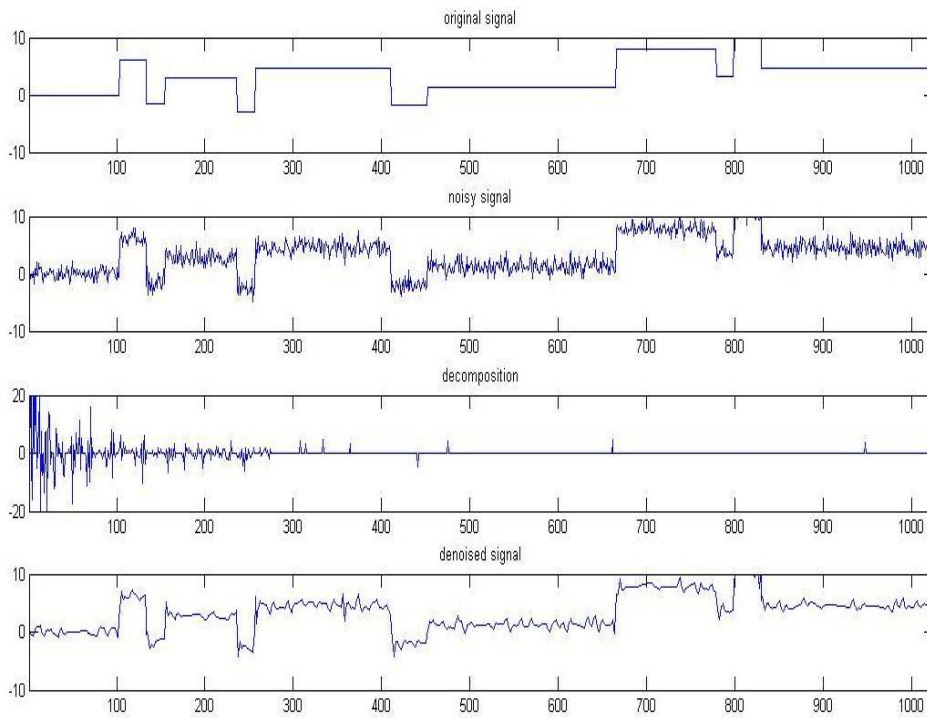


Figure 27 :Db4 wavelet transform at level 8 using hard thresholding, Heursure

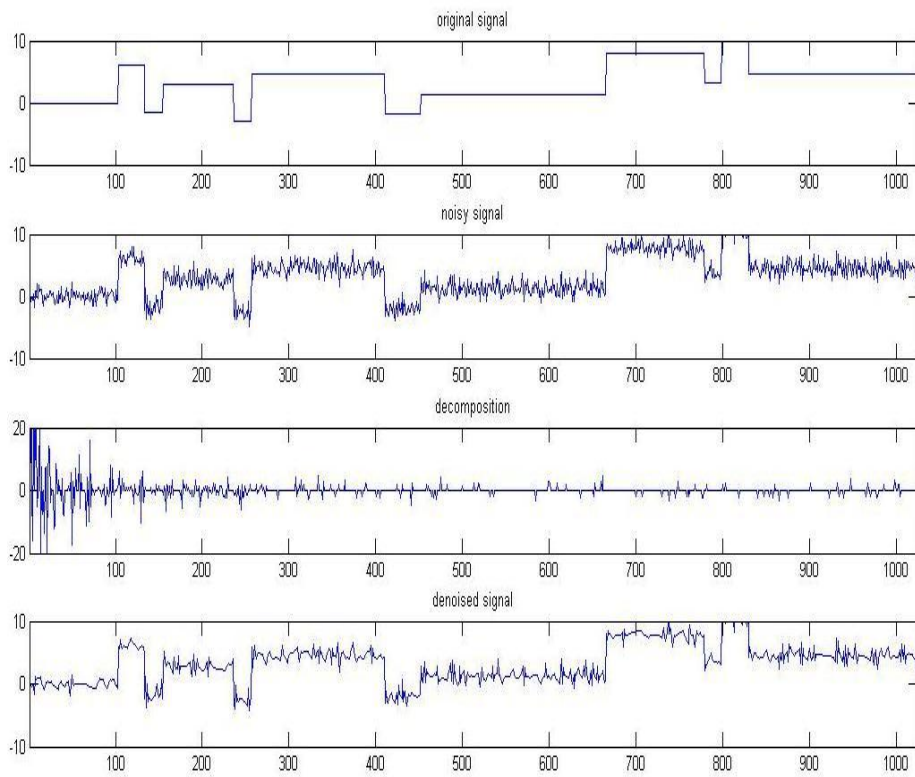


Figure 28 : Db4 wavelet transform at level 8 using hard thresholding, Rigrsure

4.1.2 Image denoising

This section deals with the comparison of two wavelet basis functions for six images that were corrupted with three types of noise. A comparative study was done using PSNR and RMSE. Denoising of tested images was carried out as explained in Chapter 3. Tables 6 to Table 8 show the overall value of PSNR and RMSE for six images with three types of noise. The yellow box indicates the highest SNR value while the green box indicates the lowest RMSE value.

Table 6: SNR and RMSE for Gaussian with variance 0.05

		Level	1	2	3
Barbara	Haar	PSNR	26.2556	27.0545	26.0879
		RMSE	12.4097	11.3192	12.6516
	Db4	PSNR	25.1366	27.2265	27.2437
		RMSE	14.1160	11.0973	11.0753
Mandrill	Haar	PSNR	26.1926	25.9412	25.7925
		RMSE	12.5000	12.8671	13.0892
	Db4	PSNR	25.6424	26.4683	26.3597
		RMSE	13.3174	12.1094	12.2618
Airplane	Haar	PSNR	26.4724	26.5642	25.9811
		RMSE	12.1037	11.9765	12.8081
	Db4	PSNR	25.6203	26.5804	27.1386
		RMSE	13.3513	11.9542	11.2101
Bridge	Haar	PSNR	26.3699	26.2644	26.1455
		RMSE	12.2474	12.3971	12.5679
	Db4	PSNR	26.0836	26.0335	26.2739
		RMSE	12.6579	12.7311	12.3835
Sailboat	Haar	PSNR	26.5623	26.4706	26.2662
		RMSE	11.9791	12.1063	12.3946
	Db4	PSNR	25.7739	26.4599	26.8372
		RMSE	13.1173	12.1212	11.6059
Couple	Haar	PSNR	26.6773	26.5022	26.0972
		RMSE	11.8216	12.0623	12.6380
	Db4	PSNR	25.8808	26.1692	25.9287
		RMSE	12.9569	12.5338	12.8856

Highest PSNR	
Lowest RMSE	

Table 7: SNR and RMSE for Salt and Pepper with variance 0.05

		Level	1	2	3
Barbara	Haar	PSNR	24.7168	25.2886	25.2351
		RMSE	14.8150	13.8711	13.9567
	Db4	PSNR	24.5985	25.1779	25.2526
		RMSE	15.0181	14.0491	13.9287
Mandrill	Haar	PSNR	25.0295	25.3107	25.2628
		RMSE	14.2912	13.8357	13.9124
	Db4	PSNR	25.1312	25.0903	25.2499
		RMSE	14.1248	14.1914	13.9330
Airplane	Haar	PSNR	24.6362	24.8575	24.8198
		RMSE	14.9531	14.5769	14.6402
	Db4	PSNR	24.5749	24.8504	24.8715
		RMSE	15.0589	14.5889	14.5535
Bridge	Haar	PSNR	24.6017	25.1477	25.2928
		RMSE	15.0125	14.0980	13.8644
	Db4	PSNR	24.3220	24.8062	24.7393
		RMSE	15.5039	14.6632	14.7766
Sailboat	Haar	PSNR	24.8168	25.1373	25.2345
		RMSE	14.6453	14.1148	13.9577
	Db4	PSNR	24.3739	24.4669	24.5585
		RMSE	15.4115	15.2474	15.0873
Couple	Haar	PSNR	24.4167	24.6912	24.7556
		RMSE	15.3358	14.8587	14.7490
	Db4	PSNR	24.0268	24.4663	24.5271
		RMSE	16.0399	15.2484	15.1420

Highest PSNR	
Lowest RMSE	

Table 8: SNR and RMSE for Speckle with variance 0.05

		Level	1	2	3
Barbara	Haar	PSNR	27.2406	27.6169	26.5179
		RMSE	11.0793	10.6095	12.0405
	Db4	PSNR	27.0892	27.3714	27.1347
		RMSE	11.2741	10.9137	11.2152
Mandrill	Haar	PSNR	27.1444	26.7270	25.9985
		RMSE	11.2027	11.7541	12.7824
	Db4	PSNR	27.0891	26.5953	26.5276
		RMSE	11.2742	11.9337	12.0270
Airplane	Haar	PSNR	27.6874	26.8234	26.1121
		RMSE	10.5238	11.6243	12.6163
	Db4	PSNR	27.4348	26.6815	27.0508
		RMSE	10.8343	11.8159	11.3240
Bridge	Haar	PSNR	26.9005	26.4576	26.0348
		RMSE	11.5217	12.1244	12.7291
	Db4	PSNR	27.6721	26.1058	26.3014
		RMSE	10.5423	12.6256	12.3444
Sailboat	Haar	PSNR	27.2940	26.8622	26.5555
		RMSE	11.0114	11.5726	11.9886
	Db4	PSNR	27.8820	27.9601	27.2011
		RMSE	10.2906	10.1985	11.1297
Couple	Haar	PSNR	27.2141	26.8375	26.6771
		RMSE	11.1131	11.6055	11.8218
	Db4	PSNR	27.3777	26.1428	25.9718
		RMSE	10.9058	12.5719	12.8218

Highest PSNR	
Lowest RMSE	

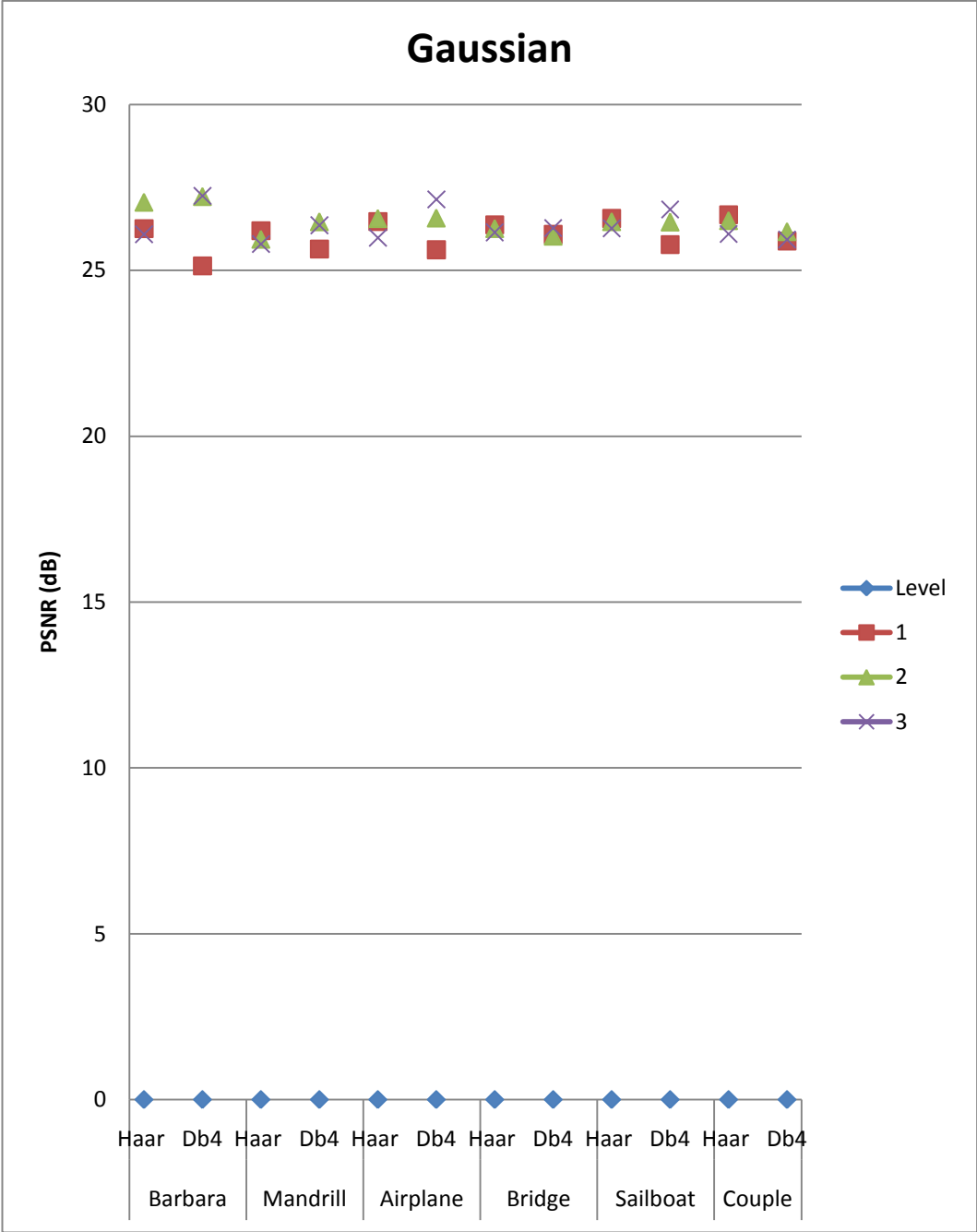


Figure 29 : PSNR vs. Images for Gaussian noise

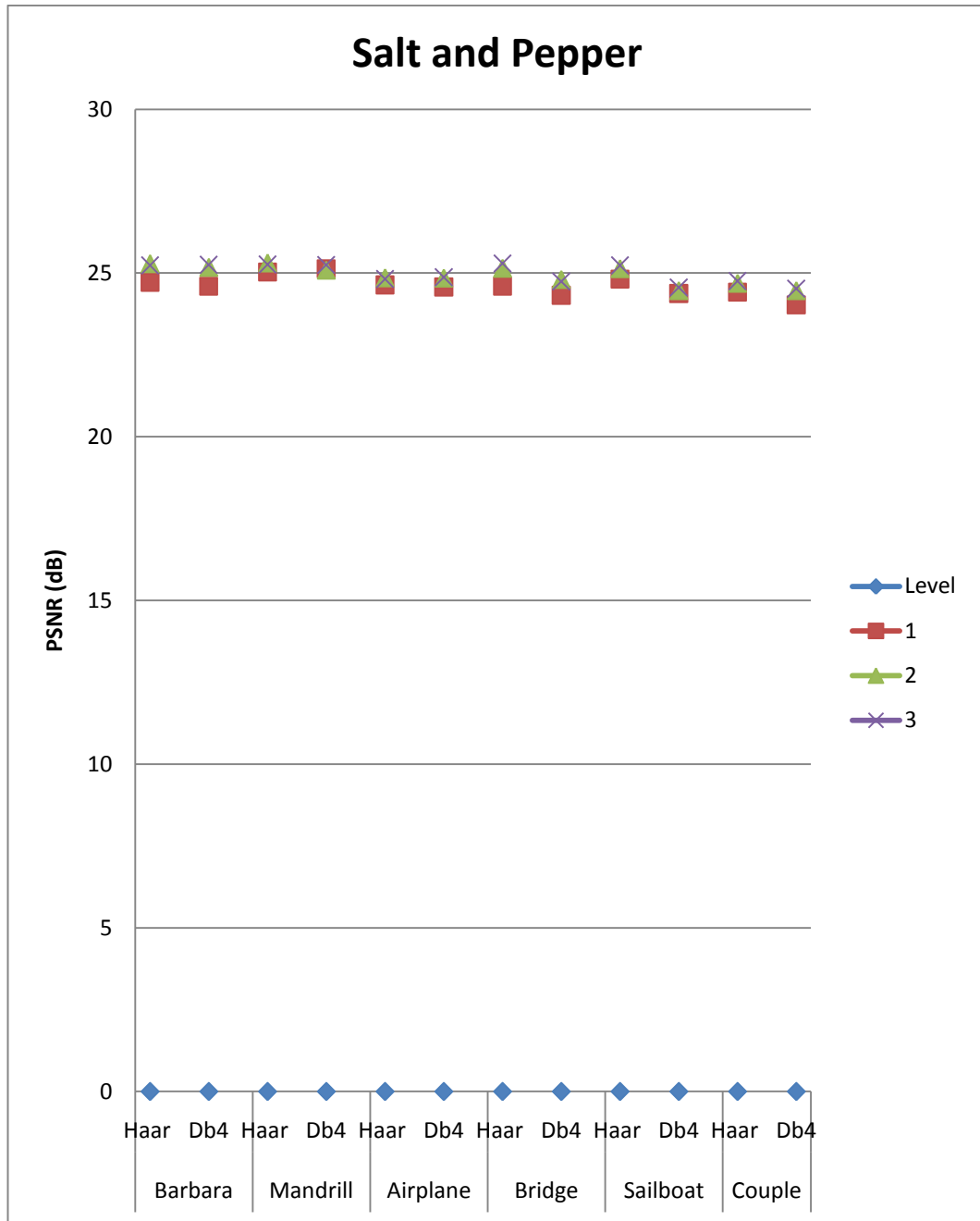


Figure 30 : PSNR vs. Image for Salt and Pepper noise

From Table 6 to Table 8, the optimum level for both Haar and Db4 wavelets can be determined. For Gaussian Noise, the optimum levels of denoising for both wavelets are at level 3 while for the Salt and Pepper noise, the optimum levels of denoising for both wavelets are at level 3. However, for speckle noise, the optimum levels of denoising for both wavelets are from level 1 to level 2.

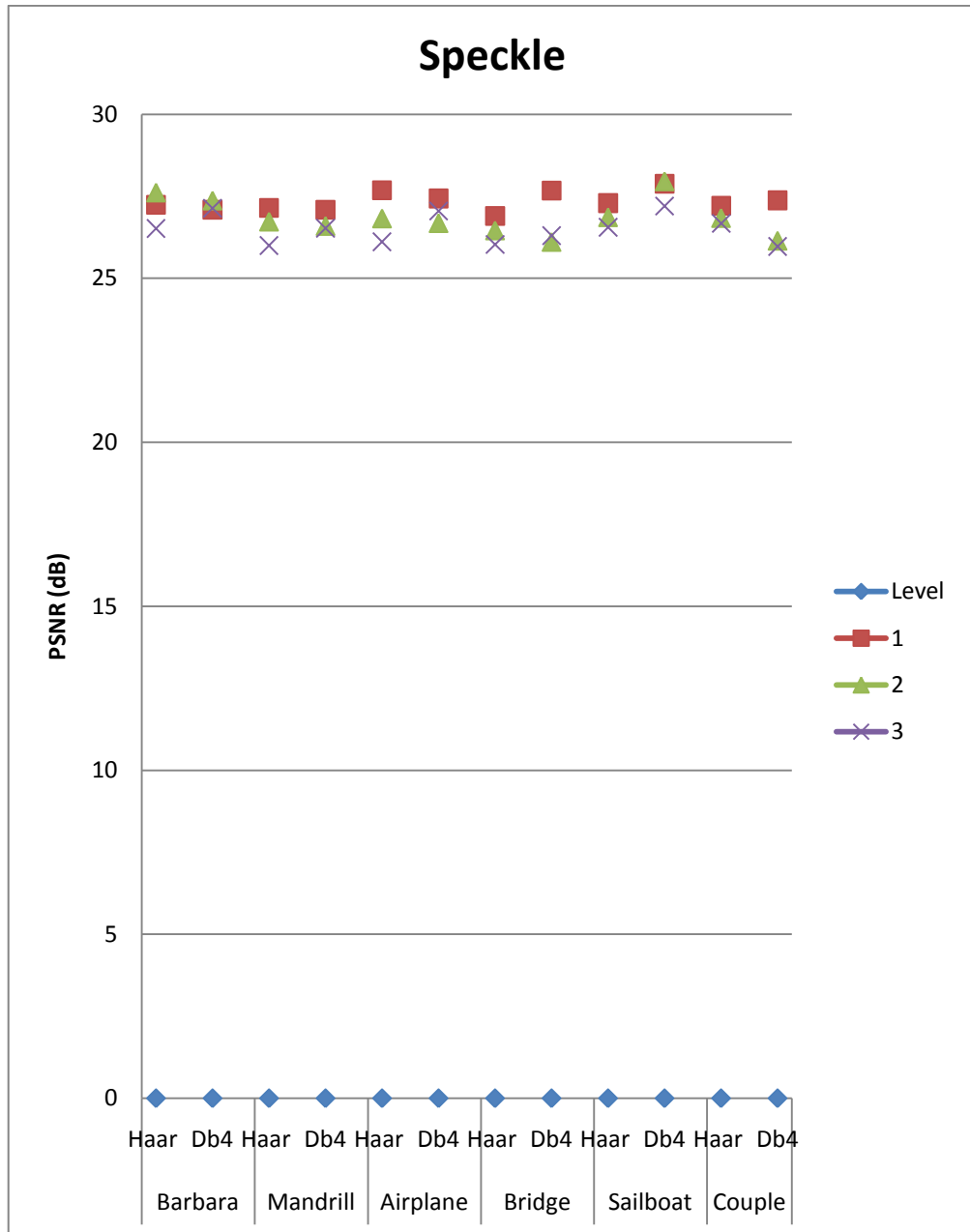


Figure 31: PSNR vs. Image for Speckle noise

As described in Chapter 3, image denoising was done in four basic steps. Firstly, the tested image was added with three types of noise. Then, wavelet transform was performed on the noisy image. Next, global thresholding was applied for every level of wavelet transform and lastly, PSNR and RMSE were calculated from level one to level three.

Denoising diagrams from Figure 32 to Figure 72 show the noisy image for the three types of noise and its respective denoised image at the optimum level of image denoising. The optimum level of denoising can be determined from Table 6 to Table 8. For image denoising, the optimum level is indicated by large value of PSNR as the overall value is not of much difference.

a. Barbara



Figure 32 : Barbara corrupted with Gaussian noise at variance 0.05



Figure 33 Denoised Barbara using Db4 at level 3



Figure 34 : Barbara corrupted with Salt and Pepper noise at variance 0.05



Figure 35 : Denoised Barbara using Haar at level 2



Figure 36 : Barbara corrupted with Speckle noise at variance 0.05



Figure 37 : Denoised Barbara using Haar at level 2

b. Mandrill

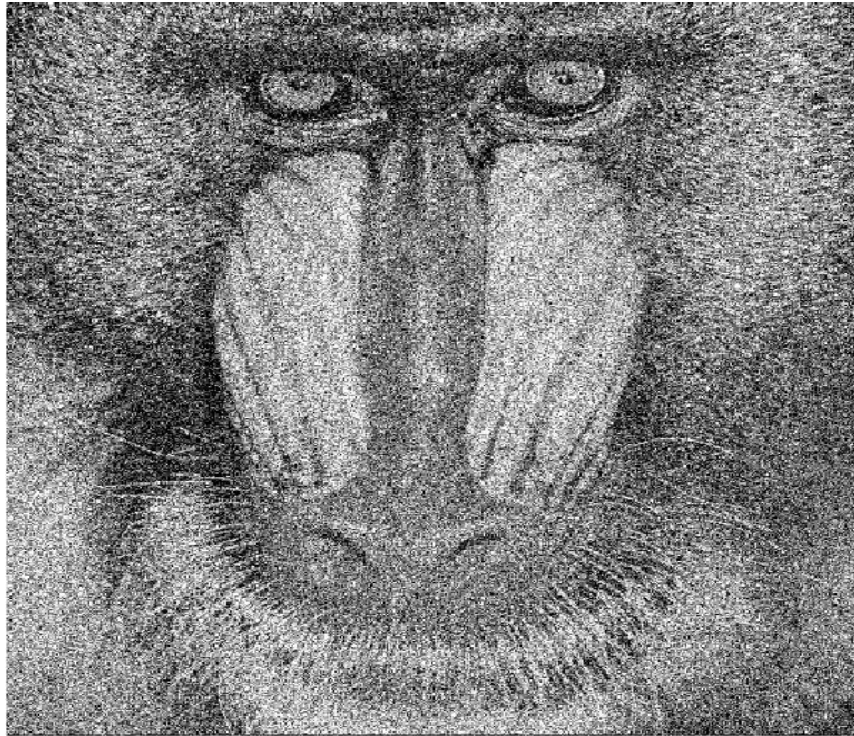


Figure 38 : Mandrill corrupted with Gaussian noise at variance 0.05



Figure 39 : Denoised Mandrill using Db4 at level 2

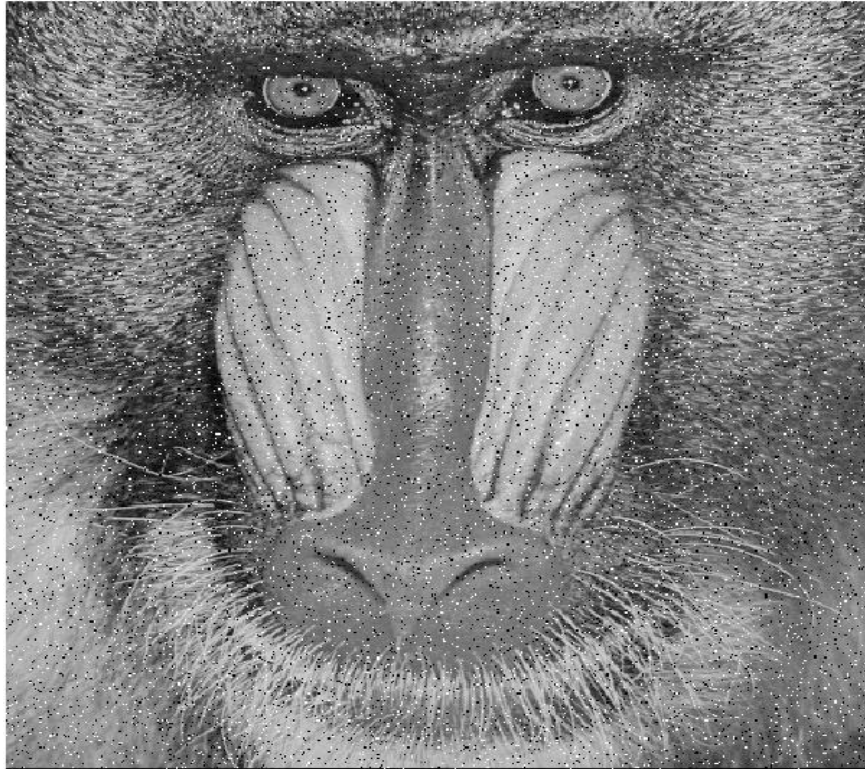


Figure 40 : Mandrill corrupted with Salt and Pepper noise at variance 0.05

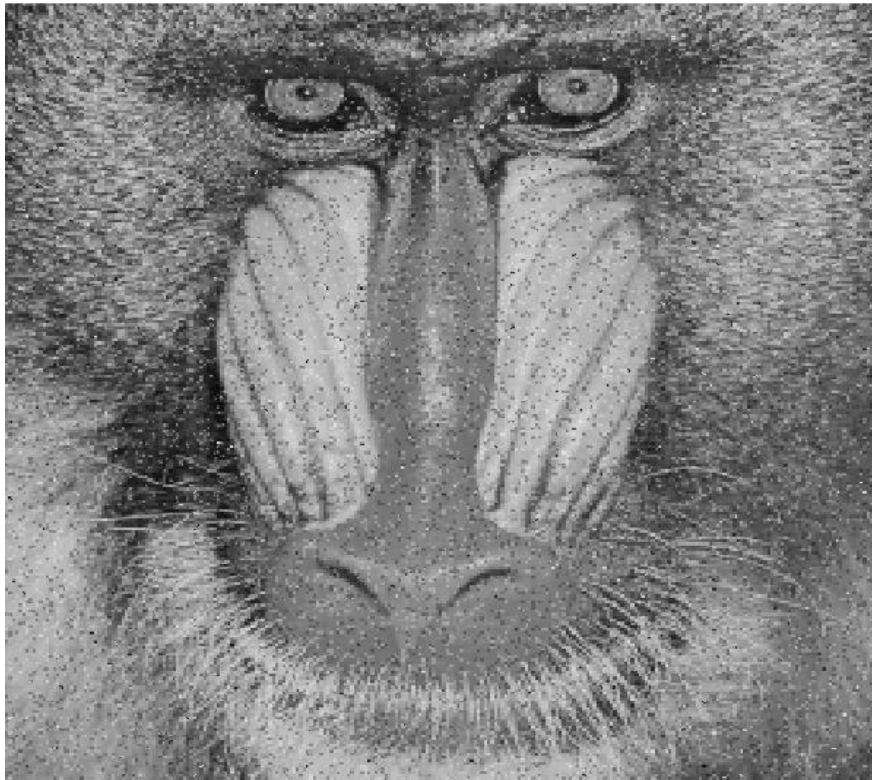


Figure 41: Denoised Mandrill using Haar at level 2

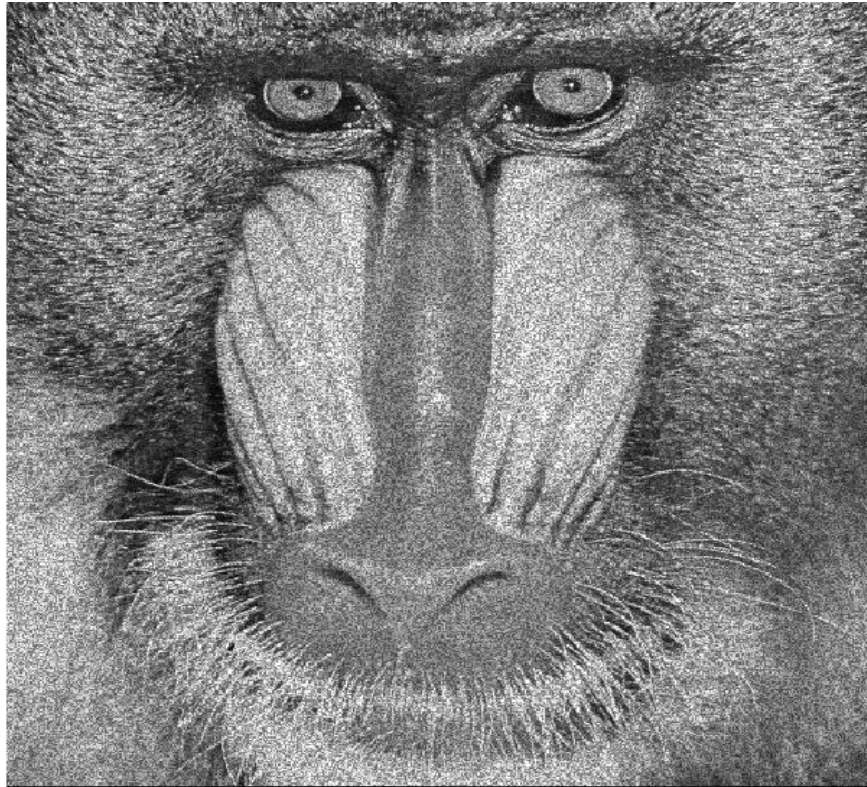


Figure 42: Mandrill corrupted with Speckle noise at variance 0.05

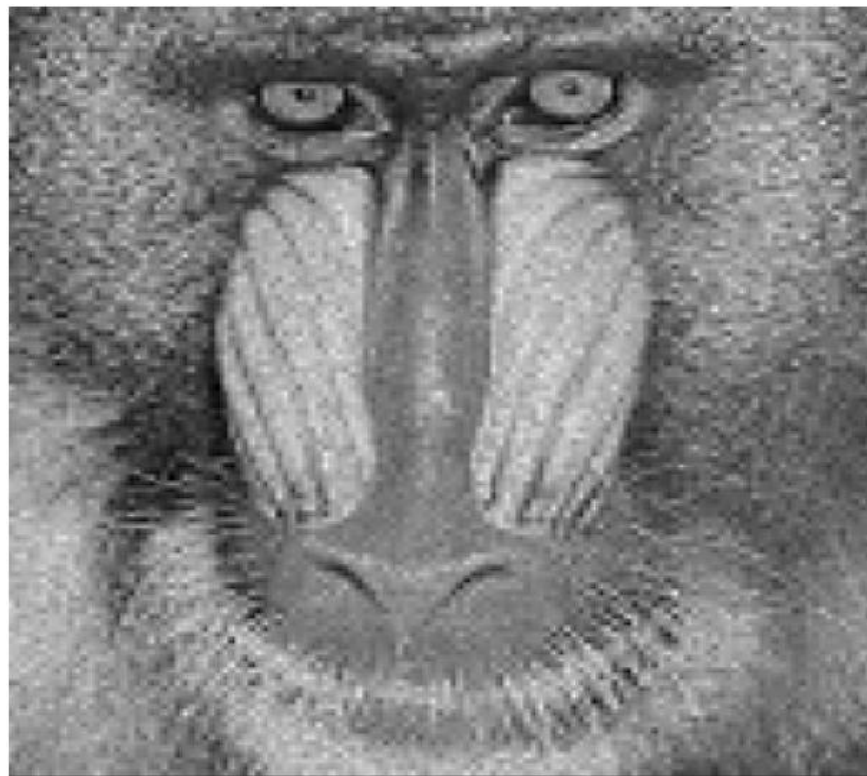


Figure 43 : Denoised Mandrill using Db4 at level 1

c. Airplane



Figure 44 : Airplane corrupted with Gaussian noise at variance 0.05



Figure 45 : Denoised Airplane using Db4 at level 3

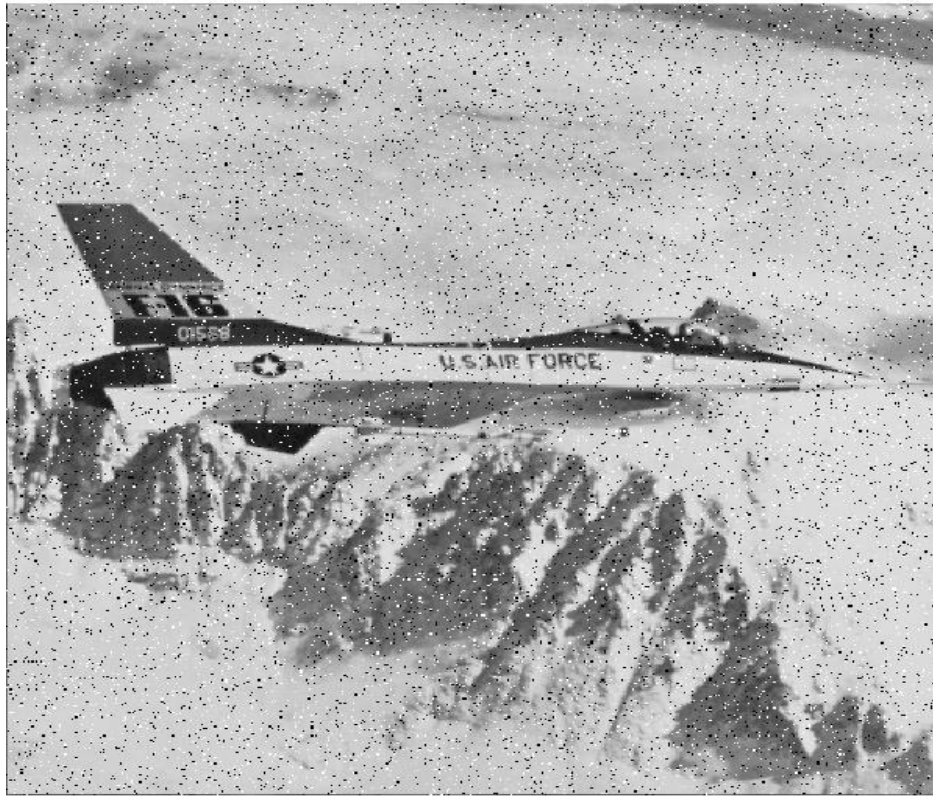


Figure 46 : Airplane corrupted with Salt and Pepper noise at variance 0.05

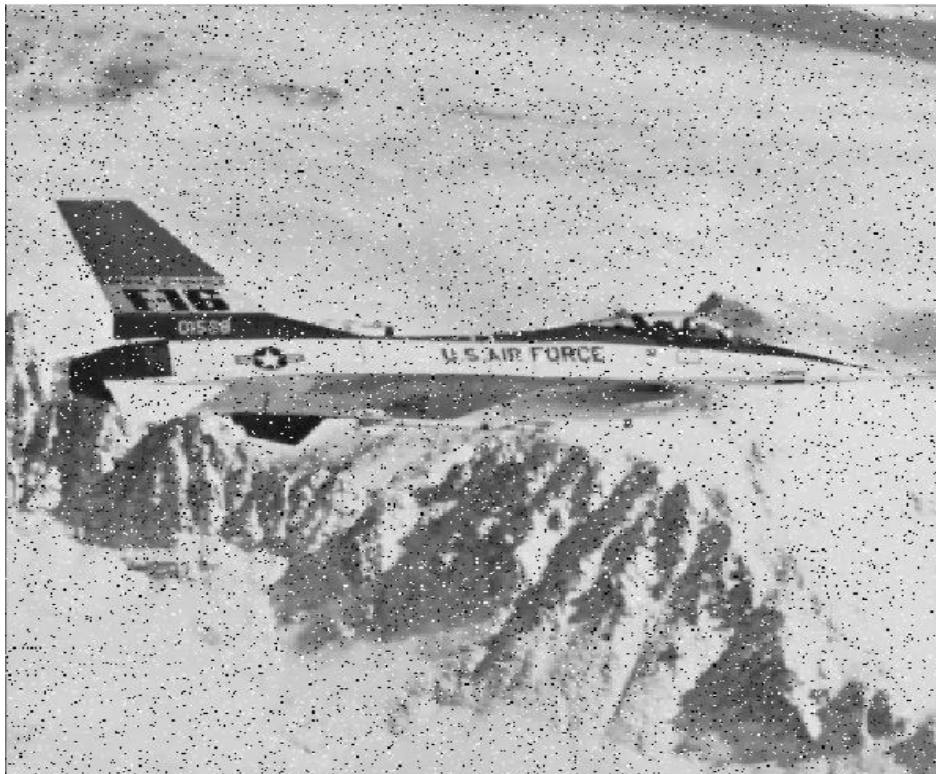


Figure 47 : Denoised Airplane using Db4 at level 3



Figure 48 : Airplane corrupted with Speckle noise at variance 0.05



Figure 49 : Denoised Airplane using Haar at level 1

d. Bridge

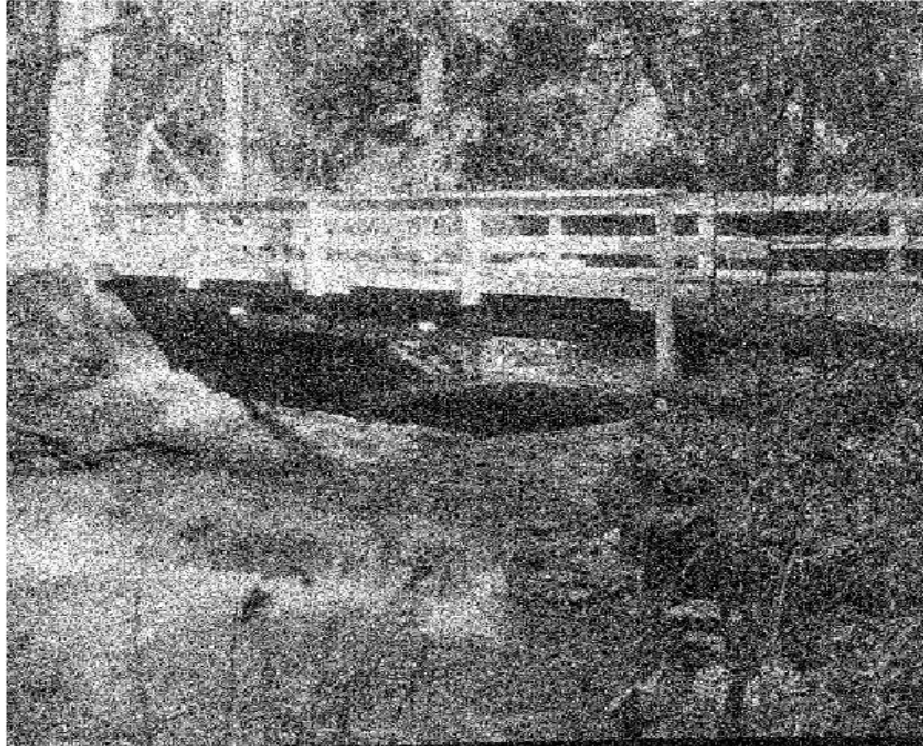


Figure 50 : Bridge corrupted with Gaussian noise at variance 0.05



Figure 51: Denoised Bridge using Db4 at level 3



Figure 52: Bridge corrupted with Salt and Pepper noise at variance 0.05



Figure 53: Denoised Bridge using Haar at level 3



Figure 54 : Bridge corrupted with Speckle noise at variance 0.05



Figure 55: Denoised Bridge using Db4 at level 1

e. Sailboat



Figure 56 : Sailboat corrupted with Gaussian noise at variance 0.05



Figure 57: Denoised Sailboat using Db4 at level 3



Figure 58 : Sailboat corrupted with Salt and Pepper noise at variance 0.05

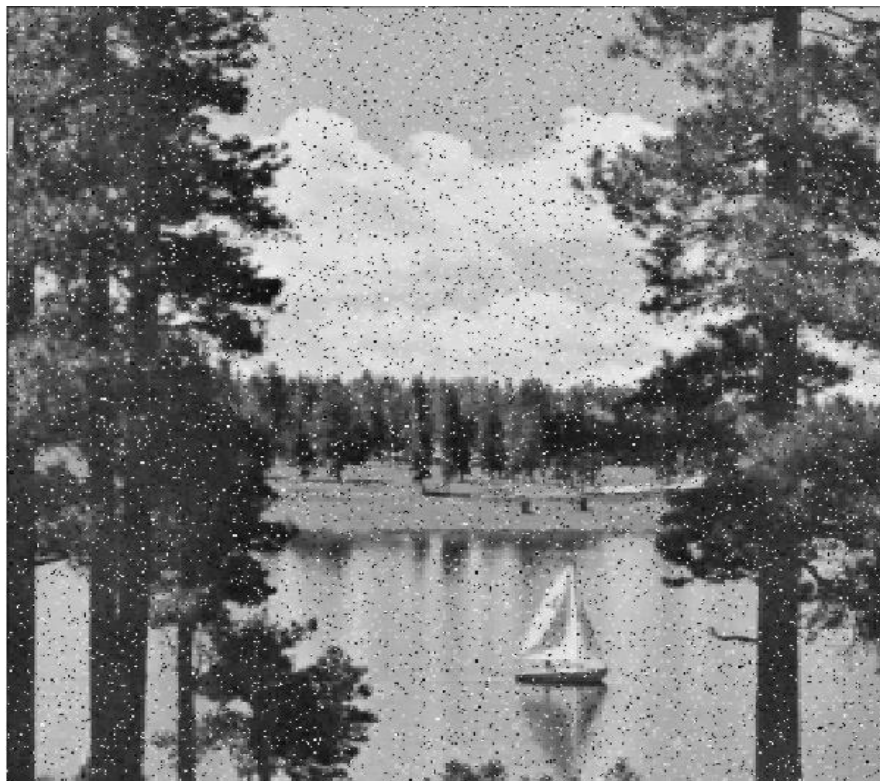


Figure 59 : Denoised Sailboat using Haar at level 3



Figure 60: Sailboat corrupted with Speckle noise at variance 0.05



Figure 61 : Denoised Sailboat using Db4 at level 2

f. Couple

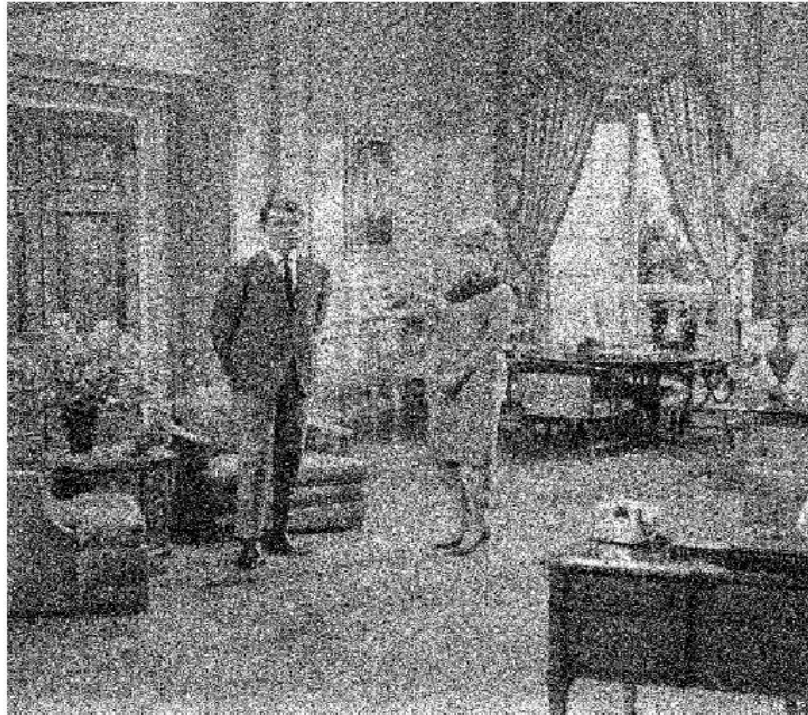


Figure 62 : Couple corrupted with Gaussian noise at variance 0.05

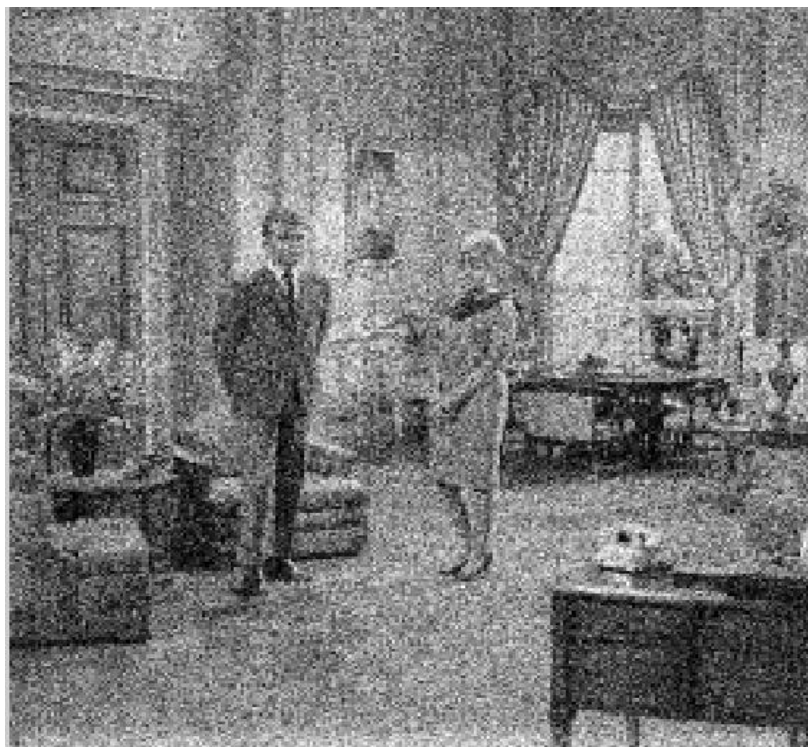


Figure 63 : Denoised Couple using Haar at level 1

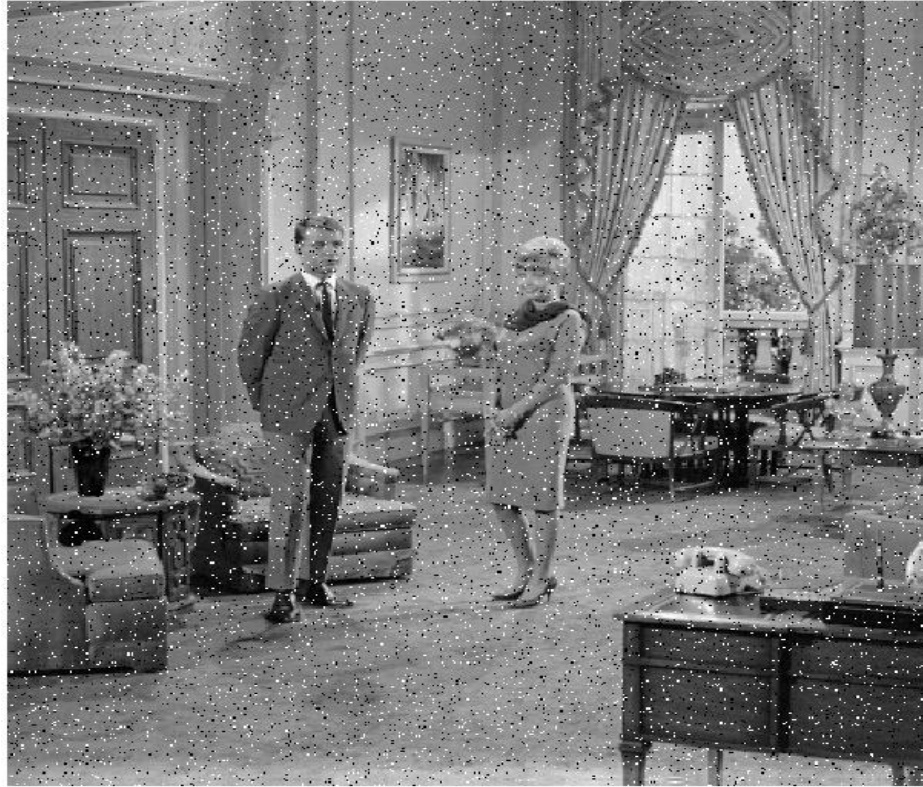


Figure 64 : Couple corrupted with Salt and Pepper noise at variance 0.05



Figure 65 : Denoised Couple using Haar at level 3

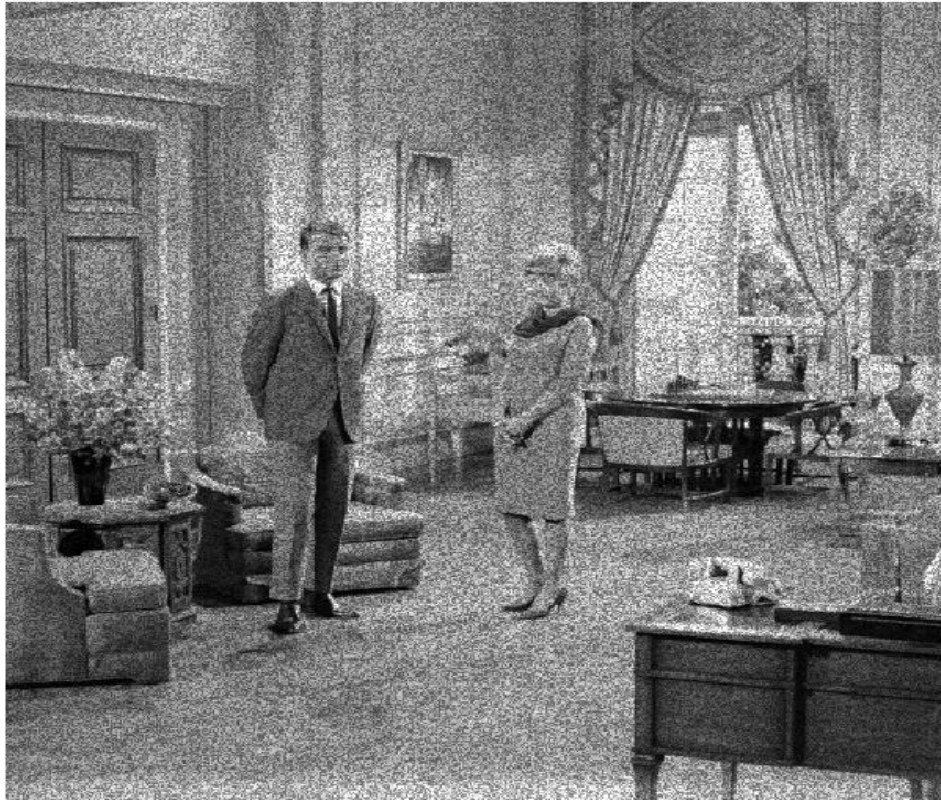


Figure 66: Couple corrupted with Speckle noise at variance 0.05



Figure 67 : Denoised Couple using Db4 at level 1

4.1.3 Kuala Lumpur Composite Index Data (KLCI)

For real application of signal denoising, data from Kuala Lumpur Composite Index (KLCI) were used as they contain many coefficients with high frequency or noise. The idea is to apply threshold value that will cut off this noise coefficient. The original data of KLCI is shown in Figure 74 below.

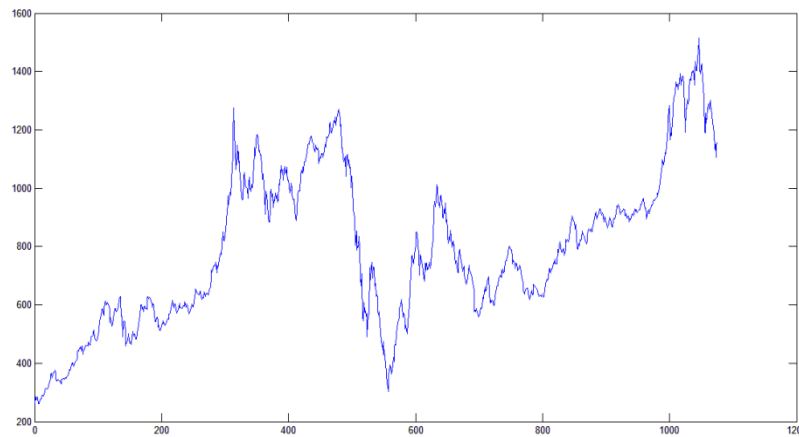


Figure 68 : Kuala Lumpur Composite Index

The same procedure used in signal denoising was applied to KLCI data except that global thresholding was used instead of Soft or Hard Thresholding. The wavelet transformation was done up to ten levels and a comparative study was done using SNR and RMSE for each level. The overall value of SNR and RMSE for 1 to 10 decomposition level is shown in Table 9 below.

From Table 9, graph of SNR and RMSE versus level is plotted in Figure 77. In Figure 75 and Figure 76, the denoised diagrams of KLCI data are shown for 10 levels of Haar and Daubechies4, respectively.

Table 9: SNR and RMSE of data KLCI

Level	1		2		3		4		5		6		7		8		9		10	
	SNR	RMSE	SNR	RMSE	SNR	RMSE	SNR	RMSE	SNR	RMSE	SNR	RMSE	SNR	RMSE	SNR	RMSE	SNR	RMSE	SNR	RMSE
Db4	38.7868	9.6192	35.7517	13.6412	33.8257	17.0251	32.6486	19.4901	32.0915	20.7771	31.8092	21.4519	31.6676	21.7959	31.5789	22.0154	31.5471	22.0967	31.5115	22.1885
	37.8925	10.6622	34.5074	15.7418	32.7892	19.1808	31.8659	21.3258	31.3848	22.5285	31.1507	23.1309	31.0396	23.4205	30.9841	23.5639	30.9539	23.6353	30.9405	23.6709
Haar	37.8925	10.6622	34.5074	15.7418	32.7892	19.1808	31.8659	21.3258	31.3848	22.5285	31.1507	23.1309	31.0396	23.4205	30.9841	23.5639	30.9539	23.6353	30.9405	23.6709
	37.8925	10.6622	34.5074	15.7418	32.7892	19.1808	31.8659	21.3258	31.3848	22.5285	31.1507	23.1309	31.0396	23.4205	30.9841	23.5639	30.9539	23.6353	30.9405	23.6709

Optimum Level	
Low RMSE	

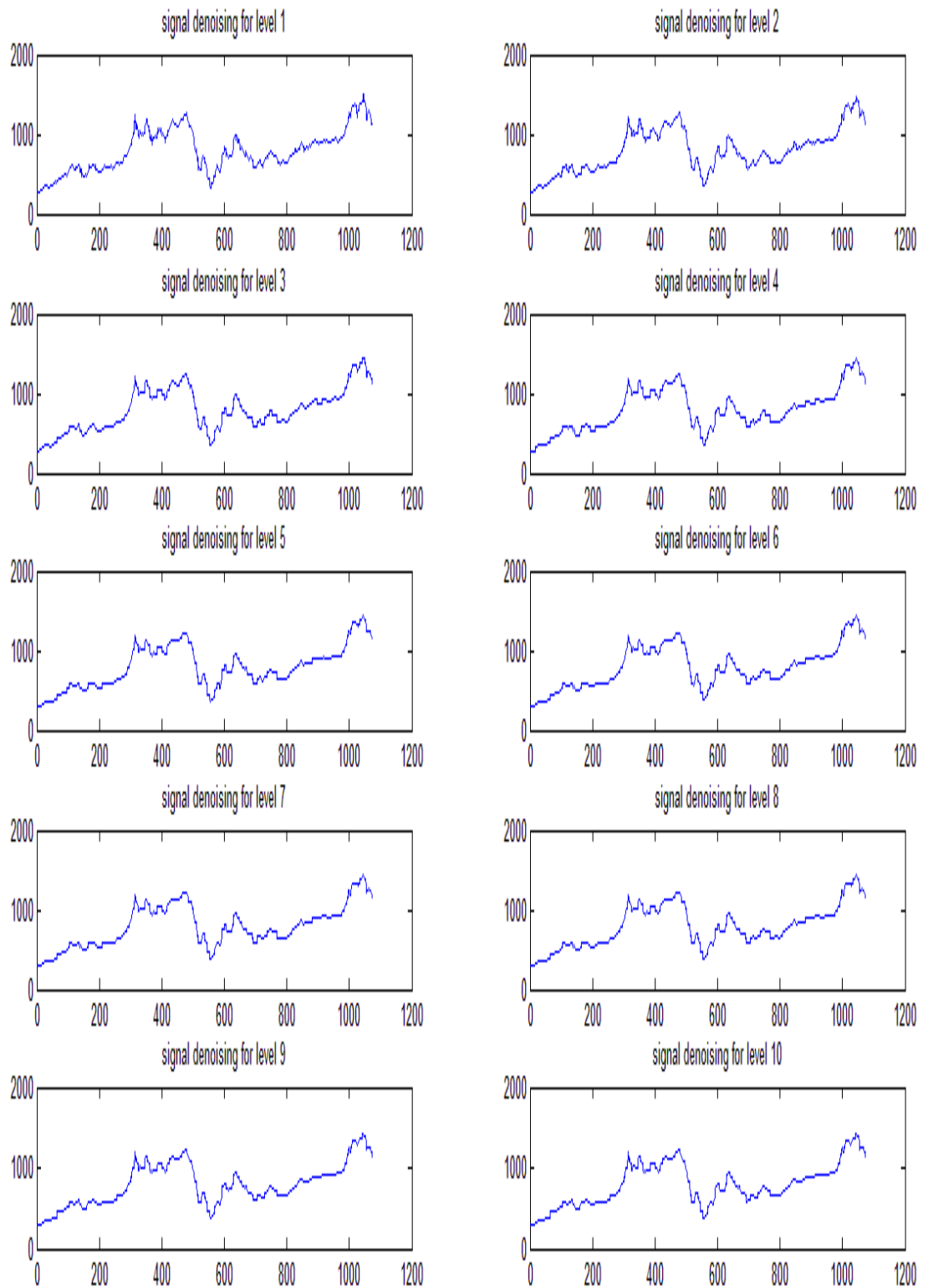


Figure 69 : Haar wavelet transform level 1 to level 10

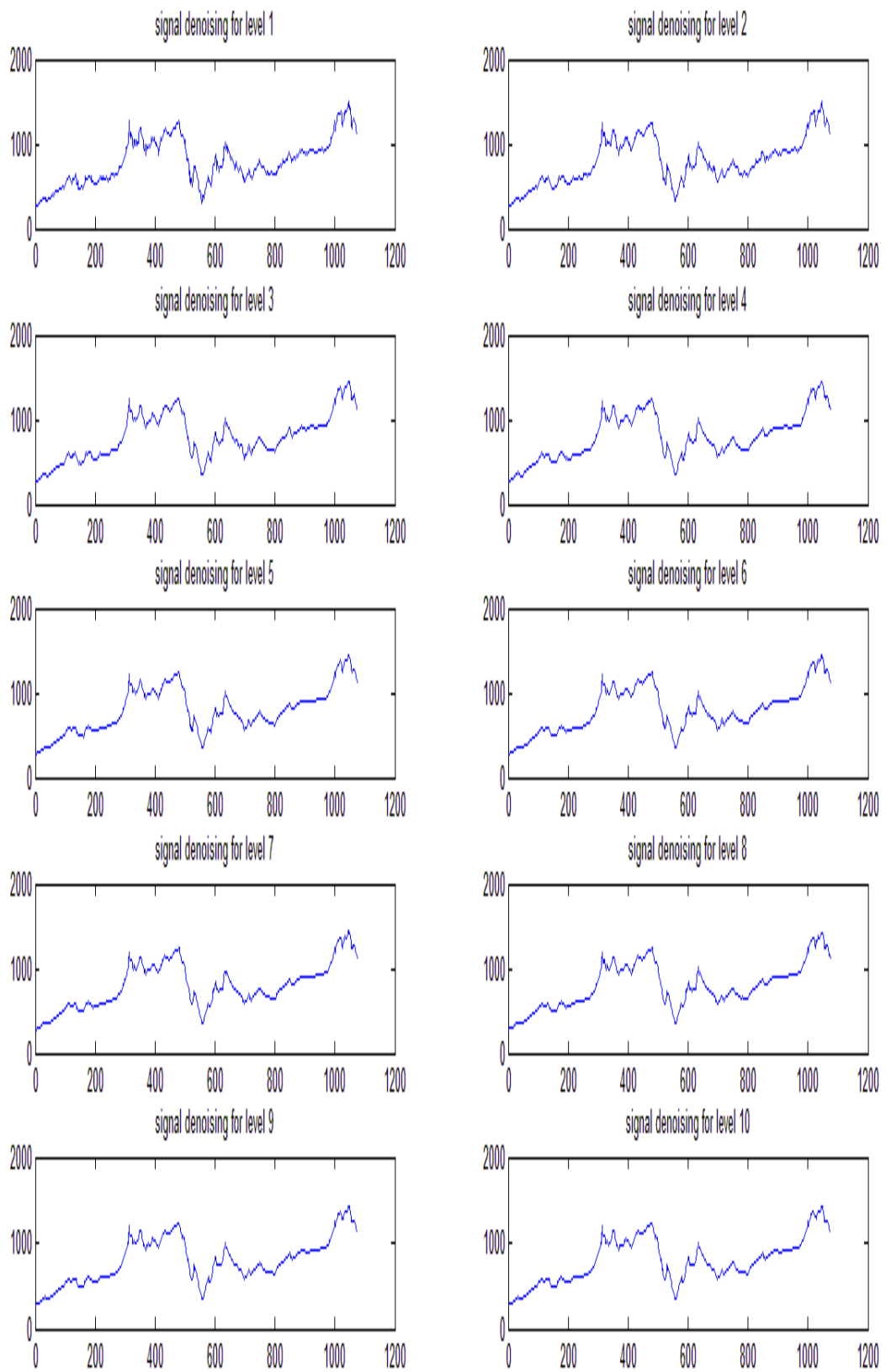


Figure 70 : Db4 wavelet transform level 1 to level 10

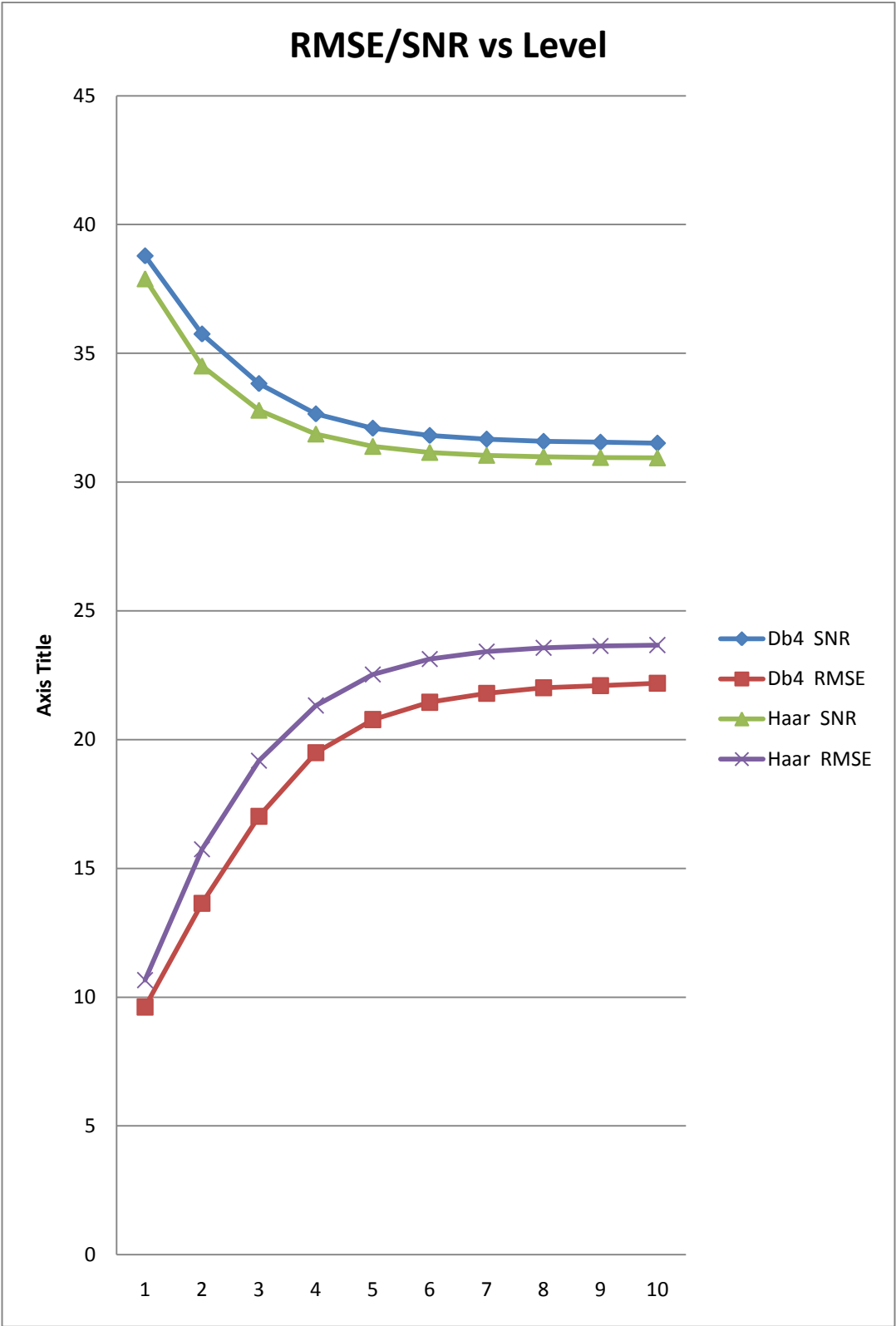


Figure 71 : The overall RMSE and SNR value vs level

4.1.4 Electrocardiography data (ECG)

Electrocardiography is one of the signals that are used to show data denoising is applicable in real application world. For this thesis, the ECG that is used is shown in Figure 78. The number of fixed length of this ECG data is $N= 1075$. For this application, global thresholding was used on the signal to filter out the high frequency of the noise from level 1 to level 6. The value of SNR and RMSE from level 1 to level 6 is shown in Table 10. The denoising diagrams of ECG data are shown in Figure 79 and Figure 80 for Haar and Db4 Wavelet basis function respectively. Again, the yellow box indicates the optimum level and the green box indicates the low RMSE

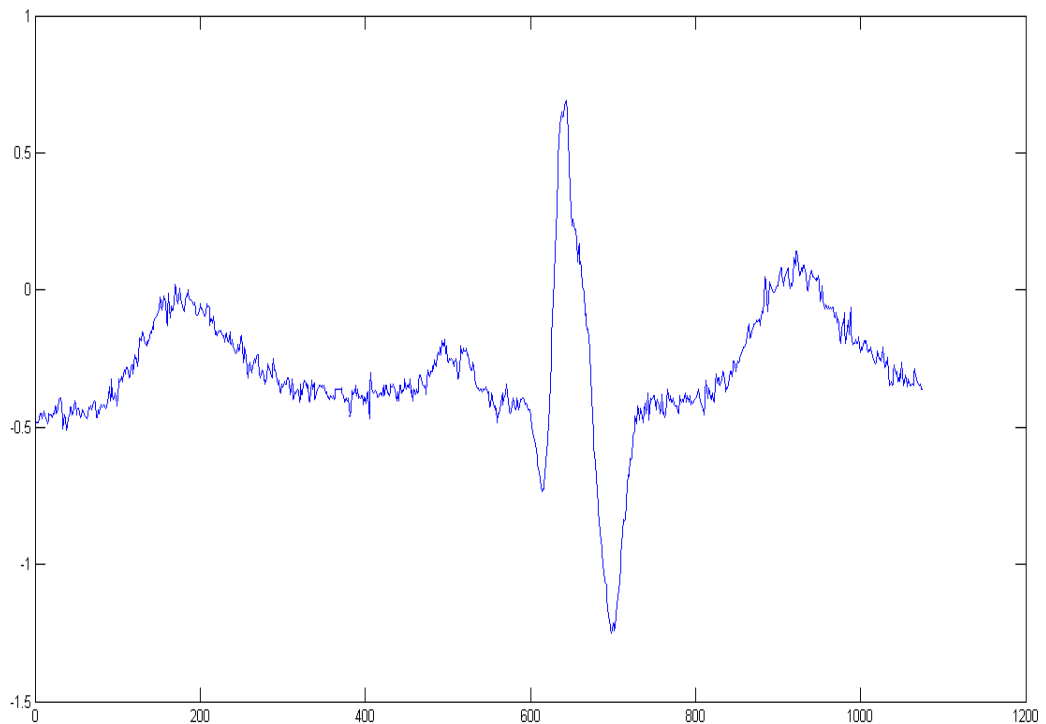


Figure 72 : ECG Data

Table 10: SNR and RMSE of ECG data

Level		1	2	3	4	5	6
Db4	SNR	29.0835	25.9581	24.2171	23.3463	22.8615	22.5849
	RMSE	0.0133	0.0191	0.0233	0.0257	0.0271	0.0278
Haar	SNR	31.1606	27.3922	25.6247	24.5109	23.9948	23.6833
	RMSE	0.0105	0.0162	0.0198	0.0225	0.0238	0.0246

Optimum Level	
Low RMSE	

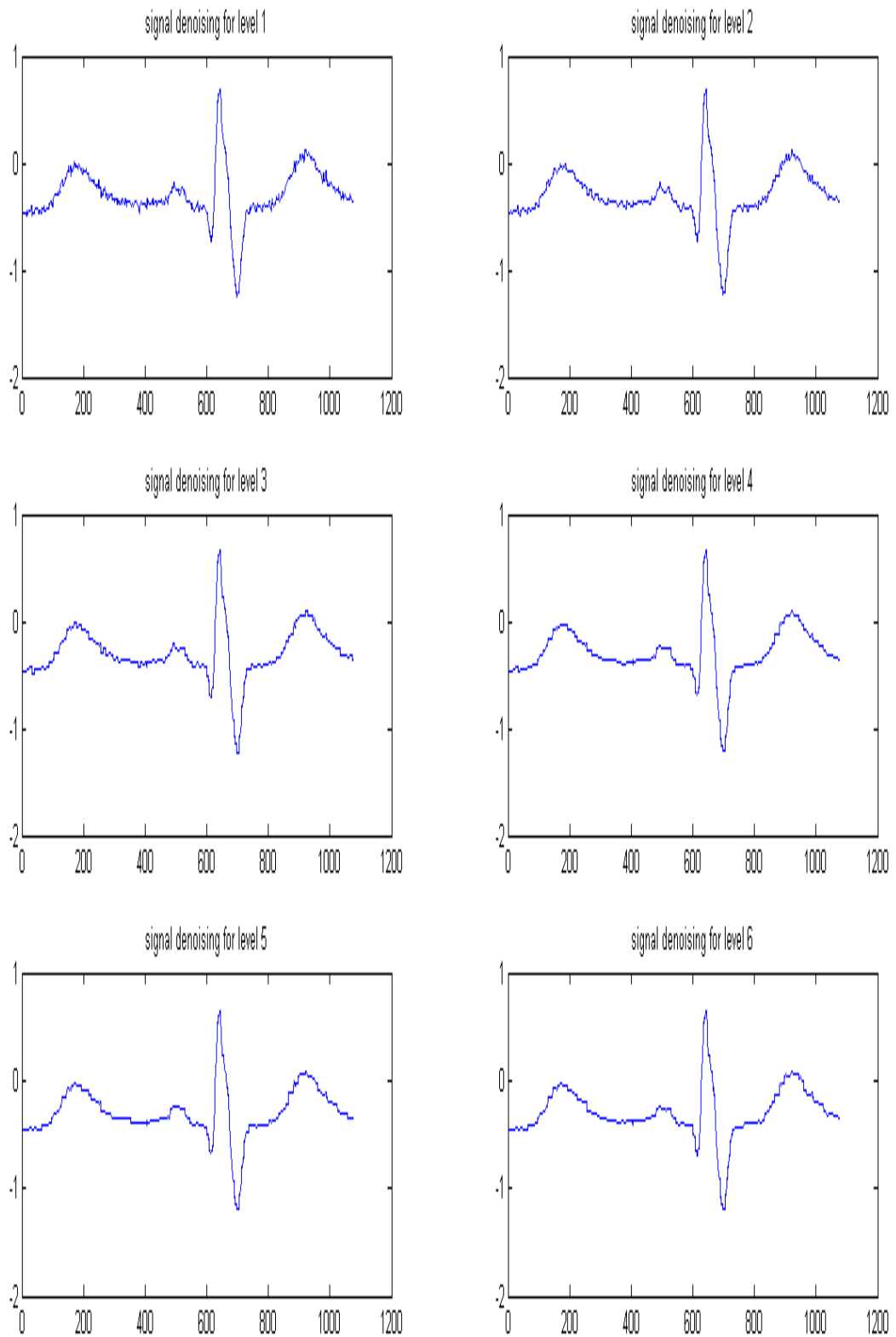


Figure 73 : Haar wavelet transform of ECG data from level 1 to level 6

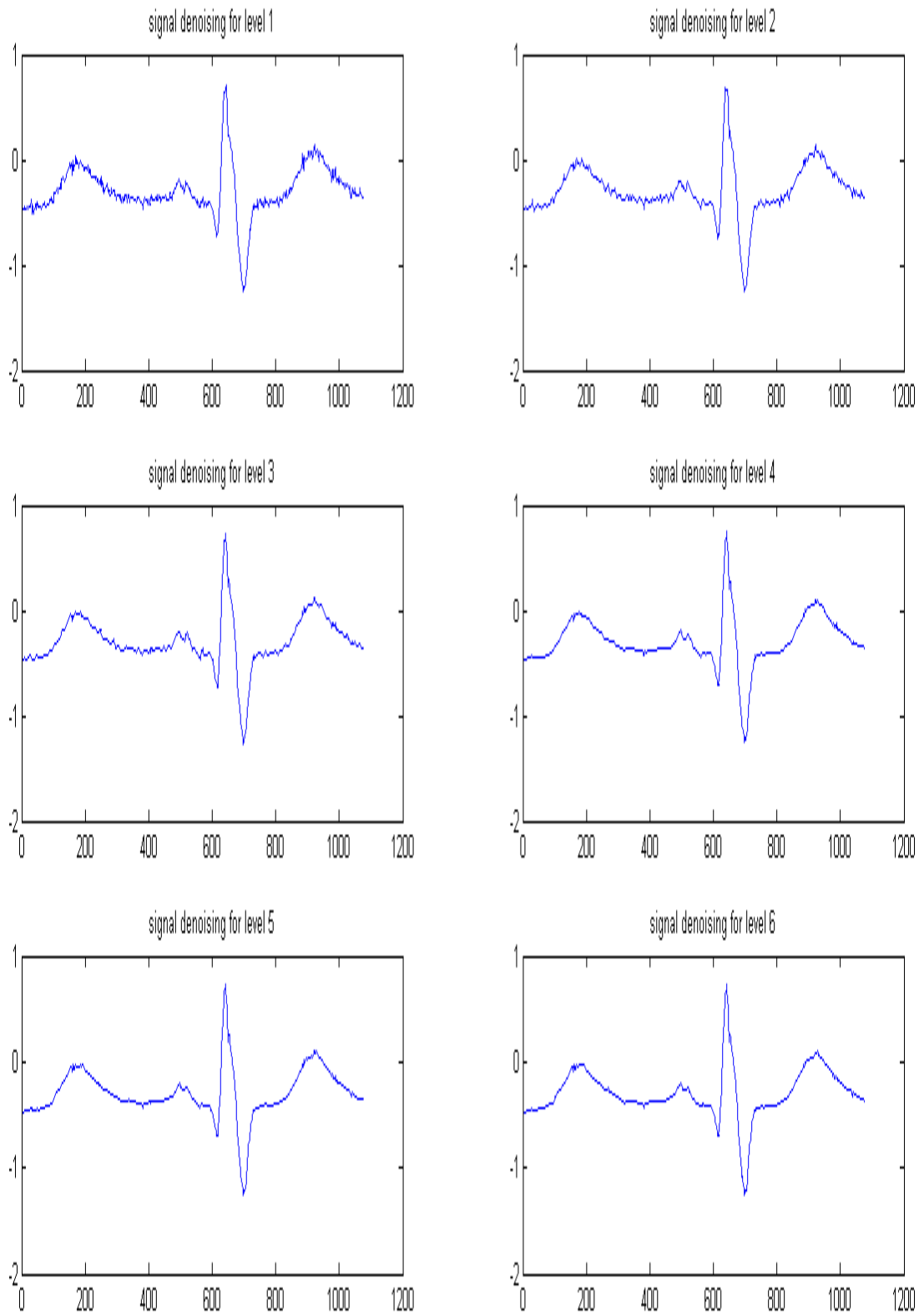


Figure 74 : Db4 wavelet transform of ECG data from level 1 to level 6

4.2 Discussions

4.2.1 Signal denoising

Table 11 below shows the overall wavelet performance of Haar wavelet and Db4 wavelet. As expected, Haar wavelet proves to be superior to Db4 wavelet for blocks signal because the structure of the blocks signal is quite similar with Haar wavelet. Therefore, the transformation and analysis of blocks signal is more reliable using Haar wavelet. For the bumps and heavy sine signals, the Db4 wavelet is better than Haar wavelet. The reason is that the Haar wavelet is not continuously differentiable which somehow makes its application limited. On the other hand, Db4 provides compact support in analyzing the tested signals and continuously differentiable. For that reason, Db4 wavelet performs better than Haar Wavelet for bumps and heavy sine signals. Notice that the optimum level of Haar wavelet is at level 10 based on the soft thresholding because the value of hard thresholding is quite scattered. However, the optimum level of Db4 wavelet is at level 8.

Table 11: Overall wavelet performance of Signal denoising

Thresholding/ signal	Soft Thresholding		Hard Thresholding	
	Heursure	Rigrsure	Heursure	Rigrsure
Blocks	Haar	Haar	Haar	Haar
Bumps	Db4	Db4	Db4	Db4
Heavy Sine	Db4	Db4	Db4	Db4

4.2.2 Image denoising

Table 12: Overall Wavelet Performance of image denoising

Gaussian with variance 0.05	Db4
Salt and pepper with variance 0.05	Haar
Speckle with variance 0.05	Db4 and Haar

From Table 6 to Table 8, we can see that for images that are corrupted with Gaussian noise, Db4 performs better than Haar with the average value of SNR is at level three. For images that are corrupted with Salt and Pepper noise, Haar is better than Db4. However for speckle noise, both wavelets performs well in image denoising. This proved that for certain data, Haar wavelet performs better than Db4 wavelet and vice versa. The overall performance of both wavelets for image denoising is shown in Table 12.

4.2.3 Kuala Lumpur Composite Index Data (KLCI)

From Table 9, the graph of SNR and RMSE versus value is plotted. We can see that as the number of level increases, the error value will increase and SNR. This is because at higher level, more coefficients will be removed, thus the difference between the original and denoised signal will be larger. Another factor that contributes to this observation is the usage of global thresholding. Global thresholding uses only one threshold value for all level of transformation. From this data also we can see that the optimum level of this transformation is at level 4 for both wavelets, and this is because starting from level 4 onwards, the SNR value becomes constantly lower. As we can see from Figure 76, most of the edges

or spikes that occur within KLCI data are preserved when using Db4 wavelet. However, using Haar wavelet as shown in Figure 75, we can see that the edges most of the time are flattened or smoothed. This shows the Db4 wavelet is flexible and thus for the denoising of KLCI data, Db4 wavelet performs better than Haar wavelet

4.2.4 Electrocardiography data (ECG)

Electrocardiography is a signal that is used in medical applications. This signal needs to be sufficiently cleaned from any noise to prevent misinterpretation from medical officer. The ECG data that are used in this thesis is shown in Figure 77. As we can see from Table 10, the optimum level is from at level 6. We can see that from level 5 to 6, the SNR value is low and start to give a constant reading. From the denoising diagrams as show in Figure 79 and Figure 80, Db4 wavelet performs better as compared to Haar wavelet, the reason is the same with KLCI data , most of edge or spike that occur within KLCI data are preserved when Db4 is used.

CHAPTER 5

CONCLUSION AND RECOMMENDATION

5.1 Conclusion

5.1.1 Signal

From the analysis of the tested signals, we can conclude that the two objectives of this project have been achieved. The optimum level of Haar wavelet for the tested signals is at level 10 while the optimum level of Daubechies4 wavelet for the tested signals is at level 8. We can also conclude that for signal denoising, Haar wavelet performs better than Daubechies4 wavelet for certain signals and vice versa. The factor that leads to this observation is the structure of the tested signals. This can be shown as in the case of the blocks signal. For the Kuala Lumpur Composite Index (KLCI and ECG), Db4 wavelet performs better than Haar wavelet. The edge of KLCI and ECG is preserved when Db4 wavelet is used and Db4 wavelet also converges faster than Haar wavelet.

5.1.2 Image

For two dimensional data, six images were used and tested with three different types of noise. For the first noise, Gaussian, we can conclude that Db4 performs better than Haar with the optimum level is at level 3. For the second noise, Salt and Pepper, Haar wavelet performs better than Db4 with the optimum level is at 1. The third noise used was Speckle noise. For speckle

noise, both wavelets give a good performance with most of the optimum level is from level 1 to 2.

5.2 Recommendation

Since selection of the right basis function plays a major role in data denoising, therefore it is important to further experiment and compare between basis functions in terms of their attributes and advantages. As a recommendation for future research, other wavelet basis functions such as Symlet, Coiflet, Biorthogonal and etc. can be used in order to give more options in selecting the appropriate algorithm in data denoising. Furthermore, as the thresholding methods that are used in this project are already established, perhaps in the future a new thresholding selection can be introduced. This thresholding selection should be a powerful threshold that filter all kind of data yet still give the optimum performance.

REFERENCES

- [1] Park “the discrete wavelet transform”, chapter 2,
<http://www.dtic.upf.edu/~xserra/cursos/TDP/referencies/ParDWT.pdf>
- [2] Hernandez-Fajardo, I.; Evangelatos, G.; Kougioumtzoglou, I.; Ming, X. Signal Denoising using Wavelet-based Methods, Connexions Web site.
<http://cnx.org/content/m18931/1.2/>, Dec 16, 2008.
- [3] Donoho, D.L and Johnstone, I.M 1994. Ideal Spatial Adaption by Wavelets Shrinkage. *Biometrika* 81: 425-455.
- [4] Mallat, S .A 1998. *Wavelet Tour of Signal Processing*, San Diego. Academic Press.
- [5] Daubechies, I. *Ten Lectures on Wavelets*. Vol.61, CBMS-NSF Reg.Con.Ser.Appl.Math.Society for Industrial Applied Maths (SIAM), Philadelphia, PA 1992
- [6] Chui, C.K. *An Introduction to Wavelets*. Academic Press, New York, 1992.
- [7] Meyer, Y. *Wavelets and Operators*, Cambridge University, Cambridge, 1992
- [8] Karim, S.A.A, Karim ,B.A. Ismail, M.T. Hassan, M.K. and Sulaiman, J . (2010). Applications of Wavelet Method in Stock Exchange Problem. Proceedings of International Conference on Fundamental and Applied Sciences (ICFAS 2010), 15-17 June 2010, Kuala Lumpur Convention Centre, 2010

- [9] Tim Edwards, “Discrete Wavelet Transforms: Theory and Implementation,” Discrete Wavelet Transforms, Stanford University, Draft #2, June 4, 1992
- [10] David L. Donoho, “De-noising by soft-thresholding,” <http://citeseer.nj.nec.com/cache/papers/cs/2831/http:zSzzSzwww-stat.stanford.edu/zSreportszSzdonohozSzdenoiserelease3.pdf/donoho94denoising.pdf>, Dept of Statistics, Stanford University, 1992.
- [11] Michel Misiti, Yves Misiti, Georges Oppenheim, Jean Michel Poggi, “Wavelet Toolbox”, (1996).
- [12] Sarita Dangeti “Denoising Techniques – A comparison”, Wavelet Transform and Denoising, May 2003, pg 22-36.
- [13] S. Grace Chang, Bin Yu and Martin Vetterli, “Adaptive Wavelet Thresholding for Image Denoising and Compression,” IEEE Trans. Image Processing, Vol 9, No. 9, Sept 2000, pg 1532-1546.
- [14] Anestis Antoniadis, Jeremie Bigot, “Wavelet Estimators in Nonparametric Regression: A Comparative Simulation Study,” Journal of Statistical Software, Vol 6, I 06, 2001.
- [15] Matlab 6.1, “Image Processing Toolbox,” .User Guide.
- [16] Scott E Umbaugh, Computer Vision and Image Processing, Prentice Hall PTR, New Jersey, 1998.
- [17] Langis Gagnon, “Wavelet Filtering of Speckle Noise-Some Numerical Results,” Proceedings of the Conference Vision Interface 1999, Trois-Riveres.
- [18] Wikipedia,thefreencyclopedia,”electrocardiography”,<http://en.wikipedia.org/wiki/Electrocardiography>

- [19] Mikhled Alfourri and Khaled Daqrouq. ECG Signal Denoising by Wavelet Transform Threshoding, American Journal of Applied Sciences 5(3): 276-281,2008

- [20] Łeski J., 1991, Detectja zespołów QRS dla zakłóconych sygnałów EKG, Post. Fiz. Mid., 26, 3-4 PL ISSN 0137-8465.

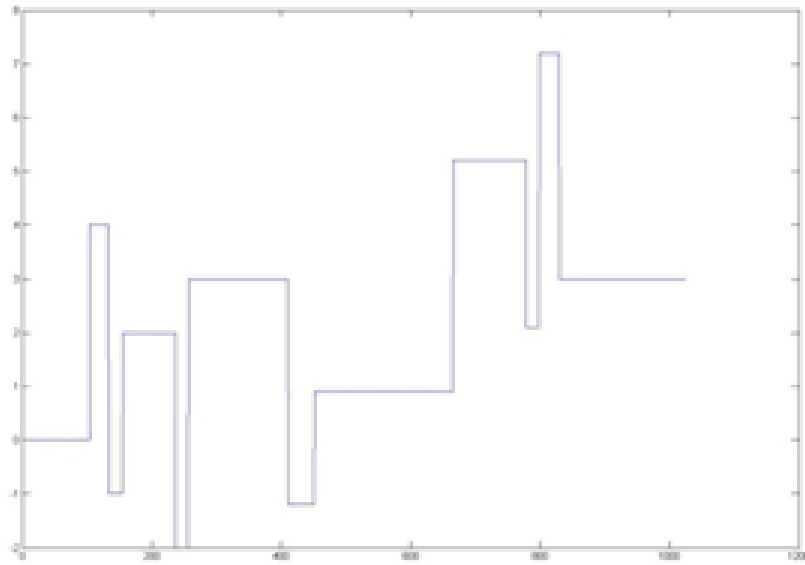
- [21] Shrouf A. 1994. The lineal prediction methods analysis and compression, PhD thesis of Slask Technical University in Gliwice.

APPENDICES

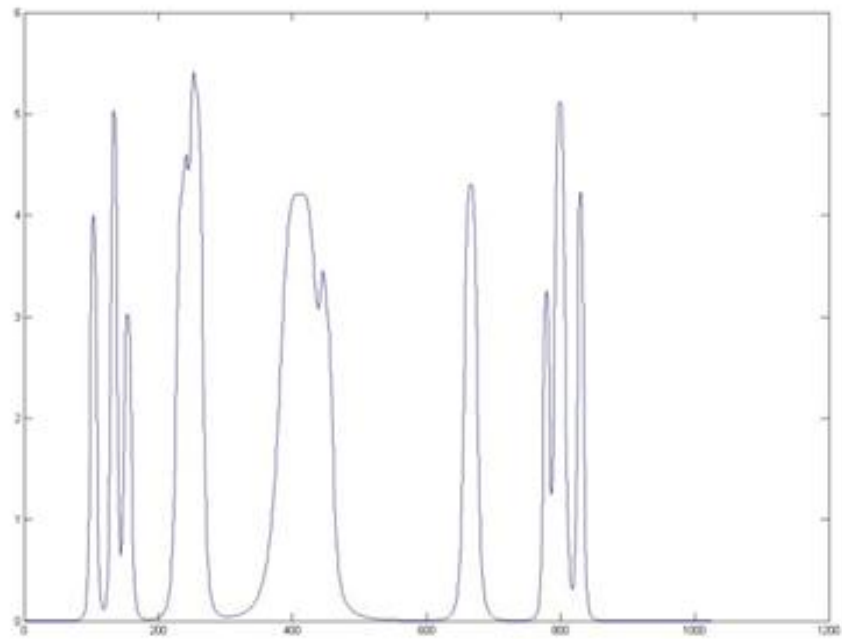
APPENDIX A

1. One dimensional data

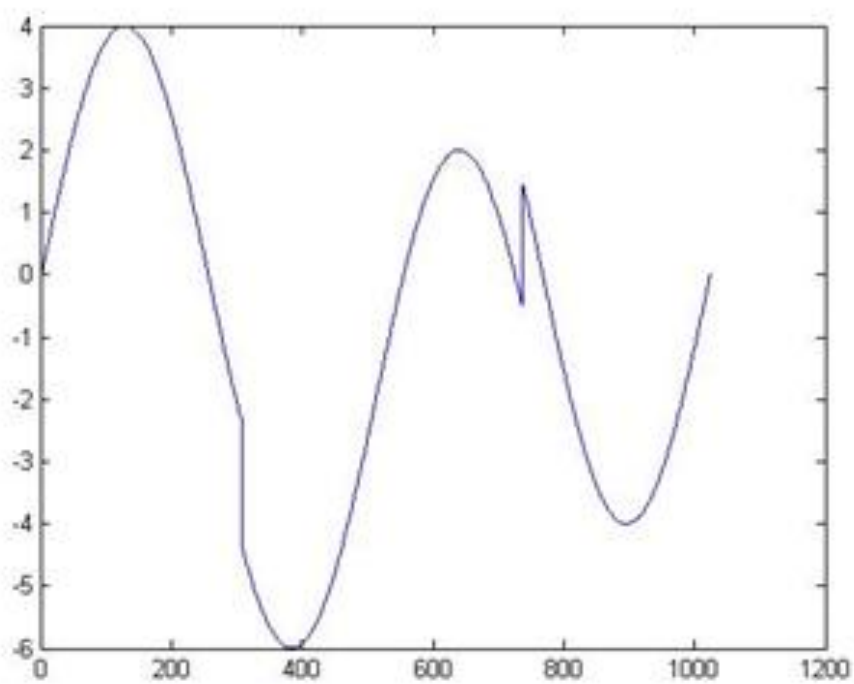
a) Blocks signal



b) Bumps signal



c) Heavy Sine signal

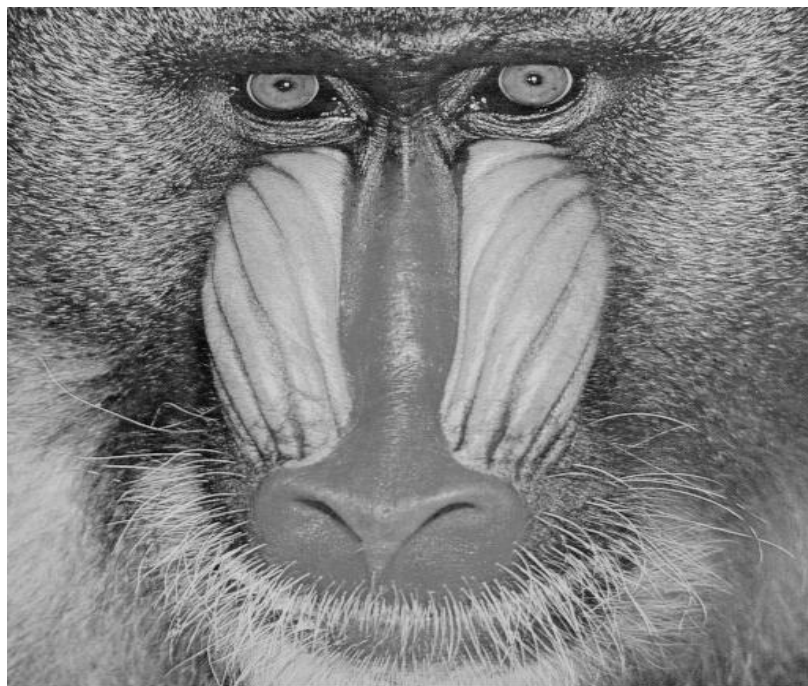


Two dimensional data

a) Barbara



b) Mandrill



c) Airplane



d) Bridge



e) Sailboat



f) Couple

